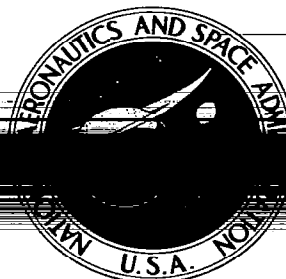
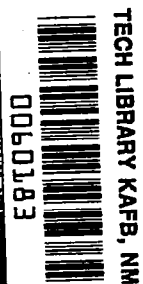


NASA CONTRACTOR



NASA CR-840



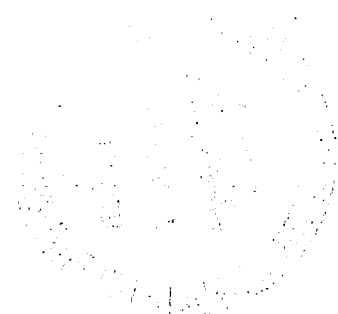
NASA CR-840

# REFRACTION OF SOUND BY JET FLOW AND JET TEMPERATURE

## EXTENSION OF TEMPERATURE RANGE PARAMETERS AND DEVELOPMENT OF THEORY

*by E. Grande*

*Prepared by*  
UNIVERSITY OF TORONTO  
Toronto, Canada  
*for*





REFRACTION OF SOUND BY JET FLOW  
AND JET TEMPERATURE

EXTENSION OF TEMPERATURE RANGE PARAMETERS  
AND DEVELOPMENT OF THEORY

By E. Grande

Distribution of this report is provided in the interest of information exchange. Responsibility for the contents resides in the author or organization that prepared it.

Issued by Originator as UTIAS Technical Note No. 110

Prepared under Grant No. NsG-661 by  
INSTITUTE FOR AEROSPACE STUDIES  
UNIVERSITY OF TORONTO  
Toronto, Canada

for

NATIONAL AERONAUTICS AND SPACE ADMINISTRATION

---

For sale by the Clearinghouse for Federal Scientific and Technical Information  
Springfield, Virginia 22151 - CFSTI price \$3.00



### ACKNOWLEDGEMENTS

The author wishes to thank Dr. G. N. Patterson, Director of the Institute for Aerospace Studies, for the opportunity to pursue this investigation.

The author is indebted to Dr. H. S. Ribner who initiated and supervised this research. His continued interest and guidance throughout the course of the work and his helpful criticism of the manuscript are appreciated.

Thanks are also due to J. Atvars and L. K. Schubert who started the experimental work and lent freely from their experience in the field, and to Dr. J. B. French, who suggested the use of a liquid nitrogen boiler to produce the low temperature jet.

The research was supported by the Air Force Office of Scientific Research, Office of Aerospace Research, United States Air Force, under AFOSR Grant No. 672-64, by the United States National Aeronautics and Space Administration, under NASA Grant No. NsG661, and by the National Research Council of Canada, under NRC Grant No. A2003.



## SUMMARY

The refraction of the sound field of an omnidirectional pure tone 'point' source of sound by the temperature and velocity fields of a 3/4" air or nitrogen jet was measured. Several different sound source positions were employed; one within the potential core of the jet, others off the axis, entirely outside the jet.

For the source in the on-axis position, the air jet velocity was varied between  $M = 0.5$  and  $0.95$  at a fixed source frequency and at ambient jet temperature, yielding a characteristic axial refraction valley. The maximum intensity reduction in the valley was of the order of 35 dB at  $M = 0.95$  and 3000 cps. in the experiment.

Using a very cold nitrogen jet ( $T = -180^{\circ}\text{C}$ ), the sound was found to be refracted inward - a focusing or channelling effect - to yield a maximum intensity along the jet axis; the maximum increased with source frequency and decreased with increasing jet velocity. At  $M = 0.112$  and 7000 cps. the intensity peak reached 26dB.

For the source in the off-axis positions, varying the air jet velocity between  $M = 0.3$  and  $M = 0.9$ , intensity polars were obtained very similar to those for on-axis source position, except for a certain skewness resulting from the non-symmetrical source position.

Jet noise polar directional plots at varying filter frequencies and jet velocities were obtained both for the air jet at ambient temperature and the nitrogen jet at  $T = -180^{\circ}\text{C}$ . These exhibited the same general shape as the polar plots for injected sound.

The jet noise polar plots in frequency bands were 'corrected' for refraction and convection to yield the approximate 'basic directivity' of the eddy sources. The refraction correction was made by adding the dB reduction in the refraction valley of the injected sound polar to the valley of the jet noise polar for the same filter frequency. The correction employed a modified Lighthill factor. At  $M = 0.3$  the 'basic directivity' in frequency bands showed good agreement with a low speed model  $a + b \cos^4\theta$  due to Ribner. At  $M = 0.9$  the agreement was only fair, due presumably to neglect of Doppler shift and other approximations.



## TABLE OF CONTENTS

		<u>Page</u>
I.	INTRODUCTION	1
II.	EXPERIMENTAL FACILITY	2
	2.1 Anechoic Chamber	2
	2.2 Pure Tone 'Point' Source	2
	2.3 Instrumentation	2
	2.4 Air Jet	3
	2.5 Low Temperature Nitrogen Jet	3
III.	EXPERIMENTAL METHODS AND RESULTS	4
	3.1 General Procedure	4
	3.2 Effect of Jet Velocity	4
	3.3 Effect of Source Position	5
	3.4 Effect of Varying Parameters for Low Temperature Nitrogen Jet	6
IV.	DISCUSSION OF RESULTS	7
	4.1 Qualitative Discussion	7
	4.2 Comparison with Simplified Theory	8
	REFERENCES	11
	APPENDIX A: Correction for Finite Microphone Size	13
	APPENDIX B: Comparison of 'Experimental' ( $\Phi_{\theta} C_{\theta}^5$ ) and 'Theoretical' ( $F(\theta)$ ) Basic Directivity	15
	FIGURES	



## I. INTRODUCTION

Subsonic jet noise has been a subject of considerable interest in the field of aerodynamic noise over recent years, and a number of theoretical investigations have been attempted. The relevant papers, e. g. 1-9, are, however, conflicting in their explanation of the axial intensity minimum in the far-field directivity pattern of jet noise. Powell<sup>5</sup> and Ribner<sup>6-9</sup> maintain that the axial intensity minimum is due to refraction of the turbulence-generated sound by the jet velocity and jet temperature fields. A theoretical investigation of this contention would necessitate solving the convected dilatation equation<sup>6, 7, 9</sup>

$$\frac{1}{c^2} \frac{\overline{D}^2 p_m^{(1)}}{\overline{D} t^2} - \nabla^2 p_m^{(1)} = - \frac{1}{c^2} \frac{\overline{D}^2 p_m^{(0)}}{\overline{D} t^2}$$

or an equivalent relation, where  $\overline{D}/\overline{D}t$  is the time derivative following the mean flow and is equivalent to  $\partial/\partial t + U \partial/\partial y_1$ ,  $p_m^{(1)}$  gives the far-field sound pressure and  $p_m^{(0)}$  is the "pseudosound" pressure. A similar equation has been solved for the highly simplified cases of idealized jets of infinite extent, without spreading.<sup>10-13</sup> The refraction thus predicted must be a great over-estimation of that for a finite jet, where the wavelengths typical of jet noise are of the same order of magnitude as the jet dimensions. The real, finite jet, however, has not yet proven amenable to quantitative analysis.

For these reasons, Atvars, Schubert and their colleagues<sup>14-18</sup> decided upon an experimental approach. Their experiment consisted of placing a pure tone 'point' source of sound within the flow field of a 3/4" air jet and observing the distortion of its inherently omnidirectional sound field. Four experimental parameters were employed: jet velocity (0.1 to 0.5 M), jet temperature (ambient to 500°F), source frequency (1000 to 7000 cps), and source position (within the jet).<sup>14, 15</sup>

The present report is concerned with experimental work done in extending the range of the parameters, in one phase to extremely low jet temperature. The turbulence-generated jet noise pattern has also been measured for a range of parameters, and in the comparison of the injected sound pattern and the jet noise pattern an attempt has been made to include theoretical developments.

## II. EXPERIMENTAL FACILITY

### 2.1 Anechoic Chamber

The measurements were made in an anechoic chamber constructed in the basement of the University of Toronto, Institute for Aerospace Studies, according to a design of J. Atvars. For details of its construction and of its free-field-simulating properties, see Ref. 14.

### 2.2 Pure Tone 'Point' Source

The 'point' source is the orifice of a 1/16" i. d. hypodermic tube coupled to an encased horn-type loudspeaker driver by a section of pipe containing a conical contraction. In order to preserve axial symmetry, the tip of the tube is bent to point directly downstream in the jet. In the absence of a jet the source radiates essentially omnidirectionally up to about 15000 cps.

The source frequency is selected on a Muirhead decade audio oscillator, the output of which is passed through a power amplifier to the loudspeaker driver unit.

For details of the tests performed on the omnidirectionality and pure-tone properties of the source see Refs. 14 and 15.

### 2.3 Instrumentation

The experimental set-up and instrumentation are shown in Fig. 1. Nearly all the instruments and controls are located in a room adjacent to the anechoic chamber. This reduces the number of sound-reflecting objects in the chamber and also facilitates operation.

The condenser microphone, an Altec Lansing type 21-BR-150 shielded by a Brüel and Kjaer windscreen, is attached to the end of a boom pivoted directly above the sound source orifice. At the frequencies considered (1000 to 7000 cps), a boom length of 76 5/8" was used, deemed sufficient for far-field measurements.

Two methods were used in extracting the pure tone signal of the source from the jet noise. For low velocity measurement ( $M < 0.5$ ) the microphone signal was passed through a General Radio sound level meter to a Muirhead wave analyzer. The analyzer served effectively as a narrow band filter with a bandwidth equal to 1.6% of the center frequency. At velocities below  $M = 0.5$  and the frequencies considered the pure tone from the source overrode the jet noise in this bandwidth. For higher jet velocities, however, this method was not applicable due to the increasing intensity of the jet noise. The microphone signal was therefore passed through the sound level meter to a Princeton Applied Research model JB-5 lock-in amplifier. A lock-in amplifier is essentially a narrow band detection system in which the incoming signal is

beat with a reference signal of the same frequency, giving a d-c output. Thus in effect it serves as a correlator, recovering the pure tone signal from the overriding jet noise. Using this method, data were obtained for jet velocities up to  $M = 0.95$ .

## 2.4 Air Jet

The air jet issues from a circular nozzle  $3/4$ " in diameter and can be operated from  $M = 0$  to  $M = 1$ . Preceding the nozzle is a heating section, containing an array of heating coils, and a settling chamber (Fig. 2). A temperature controller linked to a thermocouple in the settling chamber and to a switch in the power supply provides for automatic maintenance of a preset stagnation temperature.

The air flow is supplied by a continuously operating compressor and exhausts from the anechoic room through a  $2-1/2$  foot square duct. The velocity of the jet is determined from a manometer which indicates the difference between the static pressure in the settling chamber and the atmospheric pressure. The settling chamber pressure is adjusted by means of a control valve in the air supply line.

For further details of the jet facility and the velocity and temperature profiles of the flow see Refs. 14 and 15.

## 2.5 Low Temperature Nitrogen Jet

The nitrogen jet issues from a circular nozzle  $3/4$ " in diameter. Preceding the nozzle is a  $3-1/4$  foot long section of pipe of 8" i. d., housing a liquid nitrogen boiler and a settling chamber (Fig. 3). The boiler contains a 208 volt three-phase electric immersion heater of 7.5 KW maximum power output. The entire length of pipe was insulated by a thick layer of asbestos. The rate of evaporation of the liquid nitrogen is regulated by adjusting the power output of the immersion heater by means of a variable three-phase autotransformer. The velocity of the nitrogen jet is determined from a manometer leading to the settling chamber (cf. 2.4). The maximum jet velocity attained with the 7.5 KW heater was  $M = 0.17$  (105 ft/sec.).

The axial jet temperature at the nozzle was found to be approximately constant at  $-180^{\circ}\text{C}$  ( $-292^{\circ}\text{F}$ ) within the range of velocities used ( $M = 0.05$  to  $M = 0.17$ ), the nitrogen having been heated from the boiling point of the liquid ( $-197^{\circ}\text{C}$ ) by the walls of the settling chamber and the nozzle. The horizontal temperature profile is very nearly symmetrical around the jet axis and shows the desired temperature gradient (Fig. 4).

Due to the high density associated with its very low temperature the jet will have a 'negative' bouyancy. Therefore, on issuing into the anechoic chamber it will exhibit a droop from the horizontal plane containing the jet axis at the orifice. The droop is greatest at low velocities and approaches zero as the jet velocity is increased. When making measurements of the sound pressure level near the jet axis this effect was adjusted for by pivoting the boom vertically to find the plane of the jet. (Fig. 5.)

### III. EXPERIMENTAL METHODS AND RESULTS

#### 3.1 General Procedure

At velocities below  $M = 0.5$  the sound pressure level at the microphone, for a given source frequency and microphone position, was observed on the Muirhead analyzer decibel scale. The jet was then turned on, with the power input into the source unaltered, and the new reading on the analyzer recorded. The difference between the two readings gave the sound pressure level (SPL) reduction. The change in SPL was then normalized with respect to the value at  $90^\circ$ , since at this position there should be no appreciable change in readings for the 'jet off' and 'jet on' cases according to ray acoustics. This normalized change in SPL, observed for various angular positions of the microphone, then gave the deviation from omnidirectionality of the jet-refracted sound from the pure tone point source.

At velocities above  $M = 0.5$  the readings on the scale of the P. A. R. lock-in amplifier were maximized by adjusting the frequency and the time delay for the 'jet on' and 'jet off' positions. The ratio of the two readings, converted to decibels and normalized with respect to the value at  $90^\circ$ , gave the normalized SPL reduction.

With the point source removed the turbulence-generated jet noise was measured at various filter frequencies using the Muirhead wave analyzer. The condenser microphone-analyzer system was first calibrated, and a correction factor was applied to the analyzer readings to obtain the true SPL of the frequency band jet noise.

In all measurements except for those with the low temperature nitrogen jet, three frequencies 100 cps apart were used and the results of the three sets of measurements averaged. This procedure was employed in order to reduce scatter in the measured SPL reduction due to reflections from the walls and equipment in the anechoic chamber.<sup>14</sup>

#### 3.2 Effect of Jet Velocity

For a room temperature jet the jet Mach number was varied from 0.5 to 0.95 with the point source on the jet axis, two nozzle diameters downstream. Measurements of the SPL reduction were made at source frequencies of 2900, 3000 and 3100 cps and averaged for an effective value at 3000 cps. The angular position of the microphone was varied from  $0^\circ$  to  $90^\circ$ , and directivity patterns of the injected sound were plotted (Fig. 6).

The measured SPL reduction on the jet axis is shown in Fig. 7. It is seen that the experimental readings obtained with the lock-in amplifier show increasing deviation from the straight line indicated by the low velocity measurements made by Atvars et al.<sup>14-18</sup> This discrepancy may be explained if a cusp-like shape of the refraction valley at high jet velocity is assumed.

The measured axial intensity minimum is then the average intensity over the area of the microphone. The corrected curve in Fig. 7 was calculated by assuming the following intensity variation near the jet axis:

$$\langle p^2 \rangle \sim A + B \sqrt{\theta} + c \theta$$

The details of the calculations are indicated in Appendix A.

Similar measurements were made, varying the jet Mach number from 0.2 to 0.9, with the point source outside the jet two nozzle diameters off the jet axis and two nozzle diameters downstream (cf. 3.3). The results for this source position are shown in Figs. 8 and 9.

The turbulence-generated jet noise was measured for various filter frequencies at  $M = 0.3$ , and at velocities between  $M = 0.5$  and  $M = 0.9$  for 3000 cps. The jet noise directivity plots exhibit a shape and variation with the parameters similar to those for the injected sound (Figs. 10 and 11).

### 3.3 Effect of Source Position

The source was moved to various positions outside the jet, and measurements were made with the room temperature jet velocity varying from  $M = 0.2$  to  $M = 0.9$ , at an effective source frequency of 3000 cps. Since the microphone boom is restricted to a traverse from approximately  $0^\circ$  to  $120^\circ$  with the jet axis, the source was moved to a corresponding location across the jet axis for each source position in order to complete the traverse.

With the source kept at 2D off the jet axis, its position downstream from the nozzle was varied from 0 to 6D at a jet velocity of  $M = 0.5$ . The results obtained agree with those of Schubert<sup>15</sup>, who varied the source position downstream on the jet axis, in that there was no experimentally significant change in the SPL reduction, at any azimuthal microphone station, for the range of positions investigated (Fig. 12).

The source was now held at 2D downstream from the nozzle and its position from the jet axis varied up to 8D at a jet velocity of  $M = 0.5$ . It was found that the SPL reduction decreases in a linear manner with the distance from the jet axis (Fig. 13). At the position 2D off the jet axis, for instance, the decrease in SPL reduction is approximately 2 dB on the jet axis for  $M = 0.5$ .

A more thorough investigation was then made at the source position 2D downstream, 2D off the jet axis. The variation in directivity with jet velocity is shown in Fig. 8. As can be expected, there is a marked asymmetry, with a SPL increase  $20^\circ$  to  $50^\circ$  off the jet axis on the side of the sound source. The SPL reduction on the jet axis is shown in Fig. 9. On comparison with Fig. 7, it is seen that the refractive effect for the off-axis position is less than that for the on-axis position at all velocities for which measurements were made.

In order to investigate the asymmetry of the directivity pattern for planes other than the horizontal, the source was moved vertically and horizontally to give effectively the microphone traverses shown in Fig. 14. The directivity patterns become less asymmetric with increasing angle  $\phi$ , giving a symmetric pattern around the jet axis for  $\phi = 90^\circ$  (Figs. 15 - 18).

### 3.4 Effect of Varying Parameters for Low Temperature Nitrogen Jet

The source was kept on the jet axis, 2D from the nozzle, and measurements were made for various velocities and frequencies compensating for the droop of the jet at all microphone positions.

The directivity patterns for the cold jet show a marked difference from those for room temperature jets: a hill replaces the refraction valley. This can be explained as an intensity maximum on the jet axis due to inward refraction by the jet temperature gradient (Figs. 19 and 20).

The intensity maximum at  $\theta = 0^\circ$  for a source frequency of 3000 cps with the velocity varying from  $M = 0.05$  to  $M = 0.162$  is shown in Fig. 21. For very low velocities ( $M < 0.07$ ), the jet is very sensitive to motion of the air in the anechoic chamber, and considerable scatter in the data resulted. However, the decrease in the intensity peak with increasing velocity is clearly indicated for the higher velocities.

The source frequency was varied between 2000 and 9000 cps for a velocity of  $M = 0.078$ , and the intensity maximum on the jet axis was measured (Fig. 22). The data points show rather large scatter from the straight line drawn, but a considerable general increase of the intensity peak with increasing source frequency is apparent.

The jet noise directivity pattern was measured for  $M = 0.112$  and  $M = 0.140$  at a filter frequency of 3000 cps (Figs. 23). An intensity peak on the jet axis is exhibited, very similar to the peak found for the injected sound.

Limited tests with a jet evaporated from liquid air exhibited an intensity maximum similar to that found with the nitrogen jet.

## IV. DISCUSSION OF RESULTS

### 4.1 Qualitative Discussion

From theoretical arguments by Powell<sup>5</sup> and Ribner<sup>6-9</sup> for a jet of finite spatial extent it is expected that the spherically symmetric directivity pattern of a 'point' source of sound placed in such a jet should be distorted by refraction due to the jet velocity and temperature elevation fields to form an axial intensity minimum.

The directivity patterns of Fig. 6 show a refraction valley that widens and deepens as the jet velocity is increased. For a room temperature jet there is a reduction in SPL on the jet axis of the order of 35 dB for a source frequency of 3000 cps and jet velocity of  $M = 0.95$  (Fig. 7). Atvars et al <sup>14-18</sup> have shown that the refraction valley also deepens as either the jet temperature or the source frequency is increased (Fig. 24).

The argument could perhaps be advanced that the directivity of the jet-influenced sound from the 'point' source is due to the jet flow altering the simple source characteristics of the 'point' source. This is refuted, however, by the directivity patterns obtained for source positions entirely outside the jet (Fig. 8), which show a refraction valley only slightly less than that for source positions within the jet.

The asymmetric directivity patterns of Fig. 8 show a SPL increase approximately  $20^\circ$  to  $50^\circ$  from the jet axis on the side facing the external source. This effect, it is felt, is due to reflection of the sound waves from the side of the jet, a conclusion affirmed by the gradual return to symmetry exhibited by the directivity patterns of Figs. 15 - 18.

Moving the 'point' source laterally away from the jet axis is seen to cause a reduction of the refraction valley (Fig. 13). This result is in agreement with the concept of refraction by the jet, since the jet influences a progressively smaller part of the sound field as the source is displaced away from the jet axis.

Scattering of the sound by the random velocity and temperature gradients associated with the jet turbulence could possibly contribute to the measured effects on directivity, but this contribution must be small. Theoretically, it is noted that the acoustic wave lengths are mismatched to the turbulence scales, being much larger for the most part.<sup>19, 20</sup> Experimentally, Atvars et al <sup>14-18</sup> found that introducing a series of canted airfoil type vortex generators at the nozzle failed to make any measurable change in the directivity patterns, although a noticeable increase in the volume of the region of strong turbulence must have resulted.

The intensity maximum on the jet axis measured for the low temperature nitrogen jet (Fig. 20) is a strong refutation of the notion of appreciable directivity through scattering by turbulence. Turbulent scattering would tend to deflect acoustic energy in the same direction, regardless of jet temperature, thus causing either a maximum or a minimum in the intensity,

but not both. A more plausible explanation is that the inward refraction by the strongly negative jet temperature gradient (Fig. 4) dominates over the outward refraction by the positive jet velocity gradient to form an axial intensity maximum. This is supported by the experimental result that increasing the jet velocity decreases the height of the peak (Fig. 21), since the outward refraction by the jet velocity field would increase with jet velocity, progressively reducing the inward refraction by the cold jet temperature field.

The inward refraction by the negative temperature gradient of the jet may be more than a simple focusing process. There is the possibility that the sound waves are refracted repeatedly, successively further downstream, first from one and then from the other side of the jet such that a 'channelling' or 'wave-guide' effect takes place.

In Fig. 22 it is seen that the SPL increase with increasing source frequency does not appear to be linear. However, the sound wave lengths are of the same order of magnitude as the jet dimensions, and consequently the channelling effect may be expected to vary in a non-linear, possibly periodic manner with frequency to yield an irregular increase in SPL.

The turbulence-generated jet noise directivity contour obtained for the air jet and the strikingly different contour obtained for the very cold nitrogen jet both bear strong similarity to the respective directivity patterns for the injected 'point' source sound. It seems to be a fair inference, therefore, that refraction is a major contributor to the directional pattern of jet noise.

#### 4.2 Comparison with Simplified Theory

If ray acoustics were applicable the decibel reduction in SPL in the refraction valley of the directivity patterns for injected sound could be added to the turbulence-generated jet noise directivity contours. If this were done at corresponding temperature, velocity and frequency, the curves so obtained would approximate the jet noise polars corrected to suppress the refraction effect. (Note that source position within the jet, within limits, was found to be only a very weak parameter 14-18). Now ray acoustics is valid in the limit of small wavelengths, assuming that each ray is influenced by the points in space it passes through but independent of the surrounding field. The wavelengths typical of jet noise, however, are of the same order of magnitude as the jet dimensions, and consequently each sound ray is influenced by the entire field of the jet. The application of ray acoustics to jet noise is thus questionable, but the error is presumed to be small in the present merely comparative application where, as the later results suggest, the basic directivities (before refraction) of the injected pure tone and the jet noise sources are smooth and fairly similar over the relevant range of directions.



Ribner<sup>8, 9</sup> has developed an approximate analytic expression for the spectral density of jet noise (refraction not accounted for) that takes into consideration the variation of the convective and basic directivities with velocity and frequency. It allows for the Doppler shift of spectrum points together with an associated speculative variation in convection factor. Since the latter is considered to compensate, or overcompensate, for the Doppler shift and is unknown, a simplified version with constant convection factor and zero Doppler shift will be employed. This reads

$$\bar{\Phi}_{\theta}(f, M) \sim K \Delta f M^7 C_{\theta}^{-5} [H_{\text{self}}(f, M) + 2 H_{\text{shear}}(f, M) \cos^4 \theta] \quad (1)$$

where  $\bar{\Phi}_{\theta}(f, M)$  is the directional pattern of jet noise in a frequency band at  $f$ , as corrected to eliminate the refraction effect,  $C_{\theta}$  is the directivity factor due to convection

$$C_{\theta}^2 = (1 - M_c \cos \theta)^2 + \alpha M_c^2 \quad (2)$$

where  $\alpha$  is a constant and  $M_c$  is the eddy convection Mach number,  $2H_{\text{shear}}(f, M) \cos^4 \theta$  is the contribution of 'shear noise' and  $H_{\text{self}}(f, M)$  is the contribution of 'self-noise'.

Accordingly  $\bar{\Phi}_{\theta}(f, M)C_{\theta}^5$  may be interpreted as the directional pattern of jet noise in a frequency band at  $f$ , as corrected to suppress both refraction and (perhaps with less accuracy) convection effects. This may be termed the 'basic directivity' of the generators of the jet noise; it is called experimental if the  $\bar{\Phi}_{\theta}(f, M)$  are experimental values, and theoretical (with a symbol  $F(\theta)$ ) when Eq. (1) is employed. Since the present use (cf. Appendix B) involves a match at  $0^\circ$  and  $90^\circ$ , the comparison with the simplified theory is essentially a test to see how well the experimental 'basic directivity' fits a curve of the form  $a + b \cos^4 \theta$  with  $b/a$  of the order of unity.

The constant  $\alpha$  in the convection directivity factor is shown as 0.33, a value obtained from space-time correlations of turbulence in the mixing region of unheated air jets<sup>9, 21</sup>. The eddy convection velocity is obtained from these correlation patterns, and is chosen as  $M_c = 0.65 M$ , a value at which the turbulence intensity in the mixing region is a maximum<sup>9, 21</sup>(Fig. 25).

The experimental  $10 \log \bar{\Phi}_{\theta}(f, M)$  is obtained by subtracting the point source pattern from the turbulence-generated jet noise directivity contour to eliminate the refraction effect. The convection directivity  $10 \log C_{\theta}^{-5}$  is subtracted to yield  $10 \log (\bar{\Phi}_{\theta}(f, M)C_{\theta}^5)$ , which is then compared with the 'theoretical'  $F(\theta)$  as shown in Figs. 26 - 32.

At a Mach number of 0.3 the  $a + b \cos^4 \theta$  model from the approximate theory shows very good agreement with the experimental values for all frequencies investigated. As the Mach number is increased, however, the agreement becomes less close; at  $M = 0.9$  the deviation is approximately 4 decibels at  $\theta = 40^\circ$ . For the cold, low-velocity nitrogen jet the agreement is again satisfactory.

The discrepancy at high velocities is to be expected because the Doppler shift comes to more than a doubling of frequency, and the convection factor is so large that the variations could be significant. The neglect of these two effects implicit in (1) implies a suppression of a dependence, significant at higher speeds, of the effective  $H_{\text{self}}$  and  $H_{\text{shear}}$  on  $\theta$ . In other words, a more faithful representation of the theory than (1) is of the form  $a(\theta)+b(\theta)\cos^4\theta$ , where  $a$  and  $b$  approach constant values at low convection speeds.

## REFERENCES

1. Lighthill, M. J. On Sound Generated Aerodynamically I. General Theory, Proc. Roy. Soc. A211, 564-587 (1952), and On Sound Generated Aerodynamically II. Turbulence as a Source of Sound, Proc. Roy. Soc. A222, 1-32 (1954).
2. Lighthill, M. J. The Bakerian Lecture, 1961. Sound Generated Aerodynamically, Proc. Roy. Soc. A267, 147-182 (1962).
3. Lighthill, M. J. Jet Noise, Wright Brothers Lecture, AIAA Jour. 1, No. 7, 1507-1517 (July 1963).
4. Lilley, G. M. On the Noise from Air Jets. ARC 20, 376-N40-FM 2724 (1958).
5. Powell, A. Survey of Experiments on Jet Noise, Aircraft Engineering 26, 2-9 (1954).
6. Ribner, H. S. New Theory of Jet-Noise Generation, Directionality and Spectra, J. Acoust. Soc. Amer. 31, 245-246 (1959).
7. Ribner, H. S. Aerodynamic Sound from Fluid Dilatations - A Theory of Sound from Jets and Other Flows, University of Toronto, Institute for Aerospace Studies, UTIA Rep. 86 (AFOSR TN 3430), (1962).
8. Ribner, H. S. On Spectra and Directivity of Jet Noise, J. Acoust. Soc. Amer. 35, No. 4, 614-616 (Apr. 1963).
9. Ribner, H. S. The Generation of Sound by Turbulent Jets, Adv. in Appl. Mech., Vol. VIII, Acad. Press (N. Y. and London, 1964).
10. Gottlieb, P. Acoustics in Moving Media. Ph. D. Thesis, Physics Dept., Mass. Inst. of Tech. (1959), also Sound Source Near a Velocity Discontinuity, J. Acoust. Soc. Amer. 32, 1117-1122 (1960).

11. Moretti, G.  
Slutsky, S.

The Noise Field of a Subsonic Jet. Gen. Appl. Sci. Labs., GASL Tech. Rep. No. 150 (AFOSR TN-39-1310) (1959).
12. Slutsky, S.  
Tamagno, J.

Sound Field Distribution about a Jet. Gen. Appl. Sci. Labs., GASL Tech. Rep. No. 259 (AFOSR TN 1935) (1961).
13. Slutsky, S.

Acoustic Field of a Cylindrical Jet Due to a Distribution of Random Sources or Quadrupoles, Gen. Appl. Sci. Labs., GASL Tech. Rep. No. 281 (1962).
14. Atvars, J.

Refraction of Sound by a Jet Velocity Field, M. A. Sc. Thesis (Unpublished), Univ. of Toronto, Inst. for Aerospace Studies (1964).
15. Schubert, L. K.

The Role of Jet Temperature and Sound Source Position in Refraction of Sound from a Point Source Placed in an Air Jet. M. A. Sc. Thesis (Unpublished), Univ. of Toronto, Inst. for Aerospace Studies (1965).
16. Atvars, J.  
Schubert, L. K.  
Ribner, H. S.

Refraction of Sound from a Point Source Placed in an Air Jet. J. Acoust. Soc. Amer. 37, No. 1, 168-170 (1965).
17. Atvars, J.  
Schubert, L. K.  
Ribner, H. S.

Refraction of Sound from a Point Source Placed in an Air Jet. AIAA Paper No. 65-82, AIAA 2nd Aerospace Sciences Meeting, New York, Jan. 25-27, 1965.
18. Atvars, J.  
Schubert, L. K.  
Grande, E.  
Ribner, H. S.

Refraction of Sound by Jet Flow and Jet Temperature, University of Toronto, Inst. for Aerospace Studies, UTIAS Technical Note. No. 109 (May 1965).
19. Müller, E. A.  
Matschat, K. R.

The Scattering of Sound by a Single Vortex and by Turbulence, U. S. Air Force Office of Scientific Res. AFOSR-TN-59-337 (Jan. 1959).
20. Schmidt, D. W.

Experiments Relating to the Interaction of Sound and Turbulence, U. S. Air Force Off. of Scient. Res. AFOSR-TN-60-357 (1959).
21. Davies, P. O. A. L.  
Barratt, M. J.  
Fisher, M. J.

Turbulence in the Mixing Region of A Round Jet, ARC 23, 728-N200-FM 3181 (1962).

## APPENDIX A

### Correction For Finite Microphone Size

The directivity curves appear to approach a cusp at the minimum ( $\theta = 0$ ) as either Mach number or frequency is increased. The averaging effect of the finite microphone size can be significant over such a cusp. It is assumed that in the general vicinity of the cusp the mean square pressure ratio ( $P. R. \equiv \langle p^2 \rangle / \langle p^2 \rangle_{\text{jet off}}$ ) is of the form

$$P. R. = A + B \sqrt{\theta} + C \theta \quad (A1)$$

as measured with an ideal 'point' microphone. If the microphone subtends a small angle  $2\theta_0$  when the source-to-microphone vector  $\underline{R}$  is set at  $\theta = 0$ , then the average over the microphone face is

$$P. R._{\theta_0} = A + \frac{4}{5} B \sqrt{\theta_0} + \frac{2}{3} C \theta_0 \quad (A2)$$

On the other hand when the microphone has moved well off the cusp it is easy to justify that the average should be essentially the ideal value at the microphone center, given by (A1).

Accordingly microphone responses at three angles may be selected to give the following system of equations:

$$\begin{aligned} \theta = 0: \quad \langle P. R. \rangle_{\theta_0} &= A + \frac{4}{5} B \sqrt{\theta_0} + \frac{2}{3} C \theta_0 \\ \theta = \theta_1: \quad P. R. &= A + B \sqrt{\theta_1} + C \theta_1 \\ \theta = \theta_2: \quad P. R. &= A + B \sqrt{\theta_2} + C \theta_2 \end{aligned} \quad (A3)$$

These may be solved simultaneously to give A, the 'corrected' mean square pressure ratio at  $\theta = 0$ .

The effective diameter of the microphone was taken to include an allowance for the measured vibration due to turbulent buffeting. The data were:

microphone diameter	0.5 in.
vibration amplitude (approx.)	0.5 in.
effective diameter	1.0 in.
source-microphone distance, R	76 5/8 in.
angle subtended, $2\theta_0$	0.75°

For  $M > 0.5$  directional traverse data were available only for  $M = 0.6$  and  $M = 0.9$ . These were employed in (A3) as follows, noting that SPL reduction =  $10 \log (P. R.)$ :

<u>M = 0.6</u>		
$\theta^\circ$	SPL red. (dB) (as read)	SPL red. (dB) (corrected)
0	22.1	23.6 = 10 log A
3	19.0	19.0
5	17.9	17.9

<u>M = 0.9</u>		
0	30.2	35.5 = 10 log A
4	24.8	24.8
6	23.9	23.9

These results are exhibited in Figs. 6 and 7.

## APPENDIX B

### Comparison of 'Experimental' ( $\bar{\Phi}_\theta C_\theta^5$ ) and 'Theoretical' ( $F(\theta)$ ) Basic Directivity

Ribner<sup>9</sup> suggests the following form for the spectral density of jet noise (refraction not accounted for):

$$\frac{dP}{df} \sim \frac{\rho U_j^7 D^3}{C_\theta^5} \left[ \frac{2 H(\nu)}{C^4(\nu)} \cos^4 \theta + \frac{H(\nu/2)}{C^4(\nu/2)} \right] \quad (B1)$$

where  $\nu \equiv Cf/f^* \equiv CfD/U_j$  and  $H(\nu)$ ,  $H(\nu/2)$  are contributions due to 'shear-noise' and 'self-noise', respectively.

The experimental values of  $\bar{\Phi}_\theta(f, M)$ , the directional pattern in a frequency band at  $f$ , are readings from an analyzer with band width  $\Delta f = kf$  ( $k = 0.016$  herein). Hence:

$$\bar{\Phi}_\theta(f, M) = \frac{dP}{df} \Delta f = 0.016 f \frac{dP}{df} \quad (B2)$$

Through lack of knowledge the dependence of  $C$  on frequency as well as the Doppler shift must be neglected, resulting in the simplified, very approximate expression:

$$\bar{\Phi}_\theta(f, M) \sim K f M^7 C_\theta^{-5} \left[ 2 H_{\text{shear}}(f, M) \cos^4 \theta + H_{\text{self}}(f, M) \right] \quad (B3)$$

where  $C_\theta$  is given as

$$C_\theta^2 = (1 - 0.65 M \cos \theta)^2 + 0.046 M^2 \quad (B4)$$

upon inserting  $M_c = 0.65 M$  and  $\alpha = 0.33$  in (2).

Taking specific values of  $\theta$

$$\bar{\Phi}_{90^\circ}(f, M) = K f M^7 C_{90^\circ}^{-5} H_{\text{self}}(f, M) \quad (B5)$$

$$\bar{\Phi}_{0^\circ}(f, M) = K f M^7 C_{0^\circ}^{-5} \left[ 2 H_{\text{shear}}(f, M) + H_{\text{self}}(f, M) \right] \quad (B6)$$

Eliminating  $H_{\text{shear}}$  and  $H_{\text{self}}$  from Eqs. (B3), (B5) and (B6):

$$\bar{\Phi}_\theta(f, M) C_\theta^5 \stackrel{?}{=} F(\theta) = (\bar{\Phi}_{0^\circ} C_{0^\circ}^5 - \bar{\Phi}_{90^\circ} C_{90^\circ}^5) \cos^4 \theta + \bar{\Phi}_{90^\circ} C_{90^\circ}^5 \quad (B7)$$

Note that  $C_{90^\circ} = 1$ , thus  $\bar{\Phi}_{90^\circ} C_{90^\circ}^5 \doteq \bar{\Phi}_{90^\circ}$

The 'theoretical'  $F(\theta)$  from Eq. (B7) is compared to the 'experimental'  $\bar{\Phi}_\theta C_\theta^5$  as exhibited in Figs. 25 - 32.

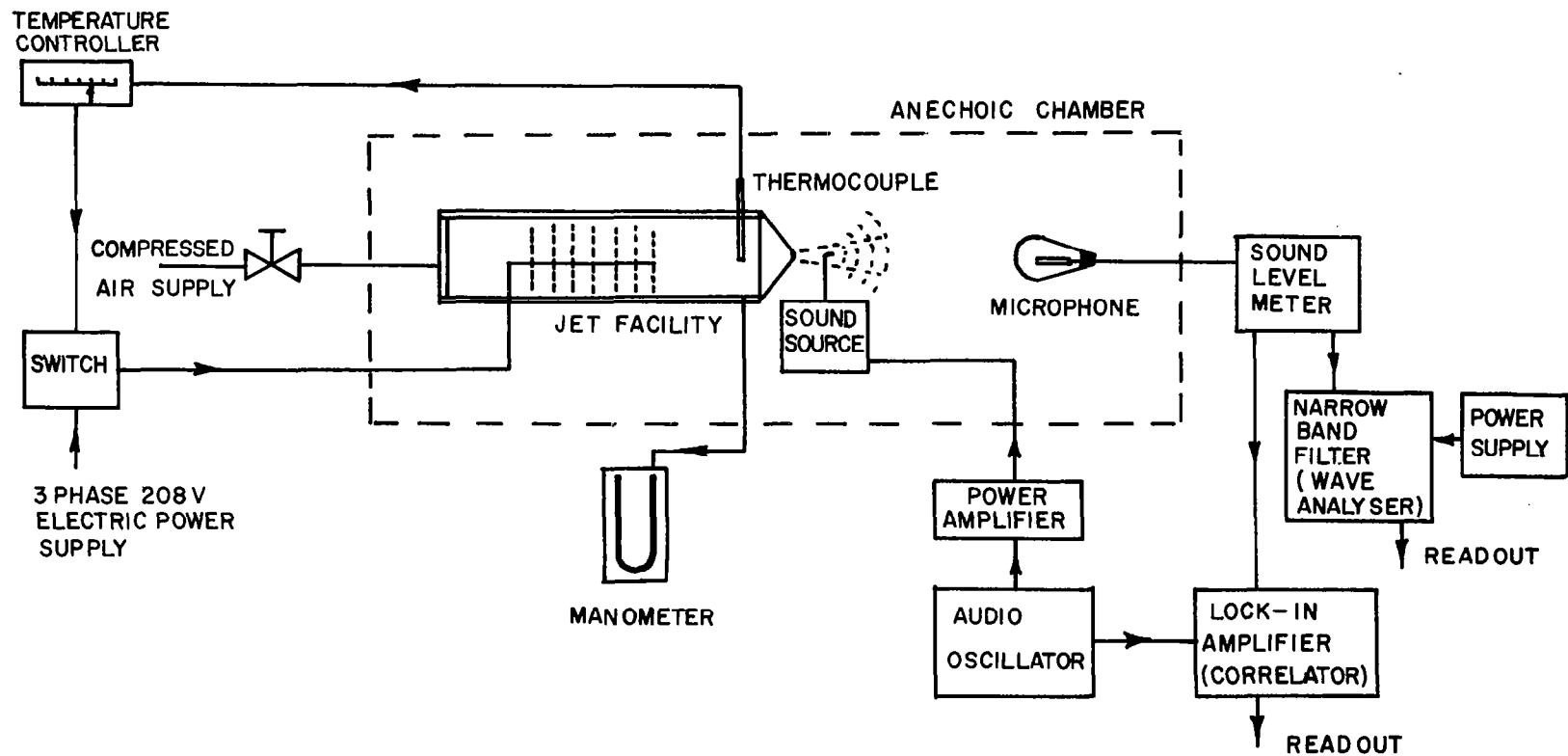


FIG. 1. EXPERIMENTAL ARRANGEMENT



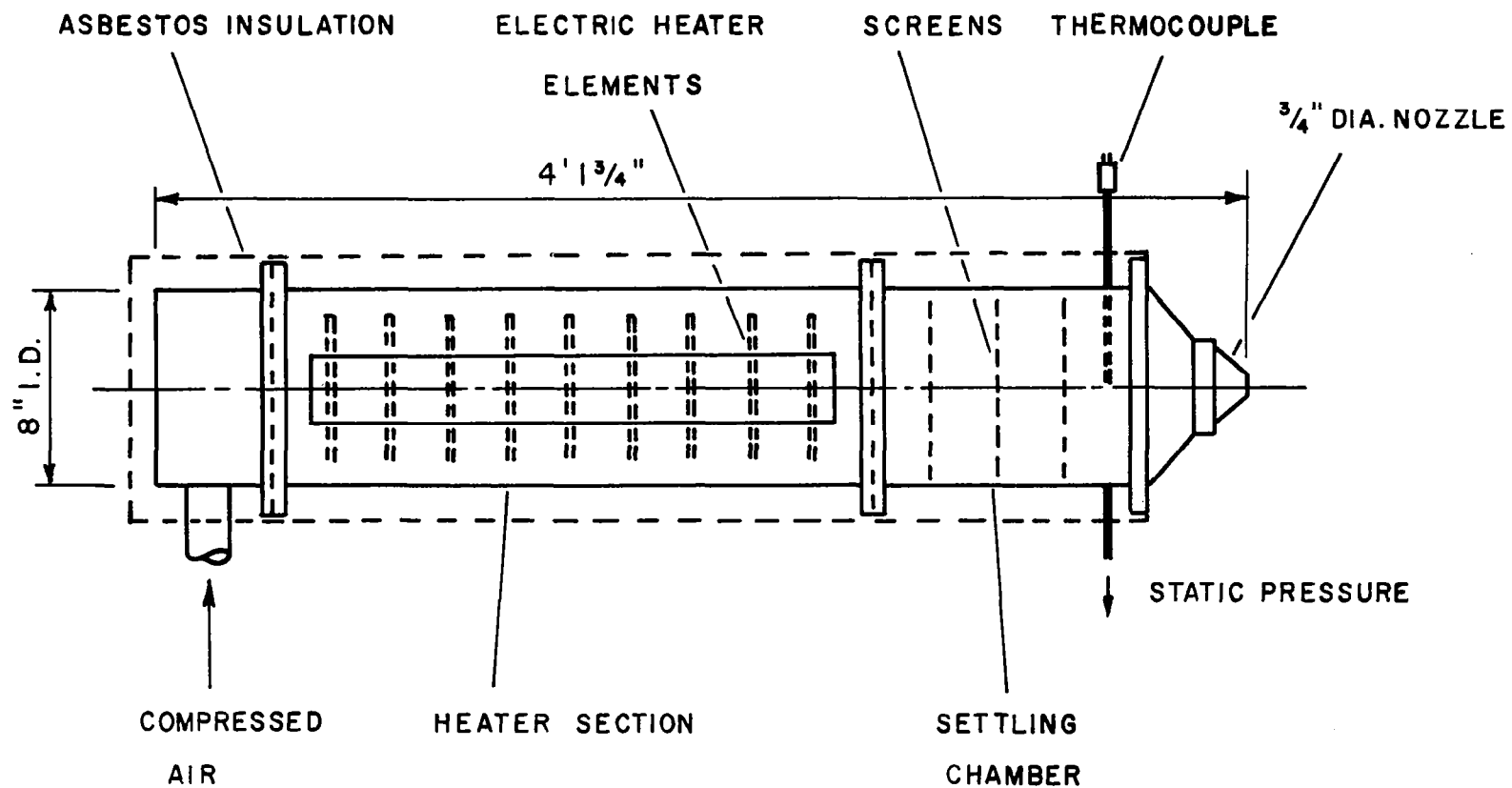


FIG.2. AIR JET FACILITY

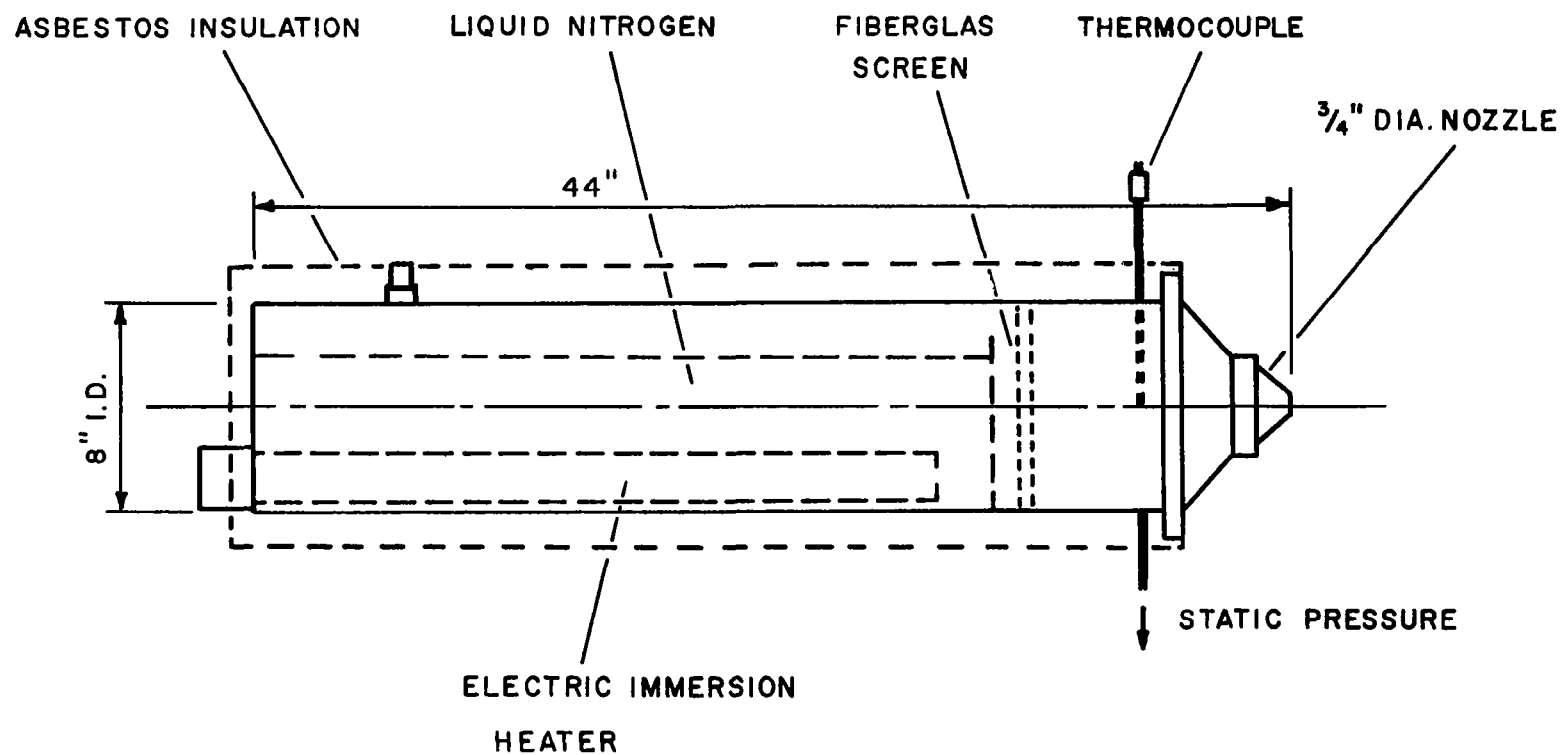
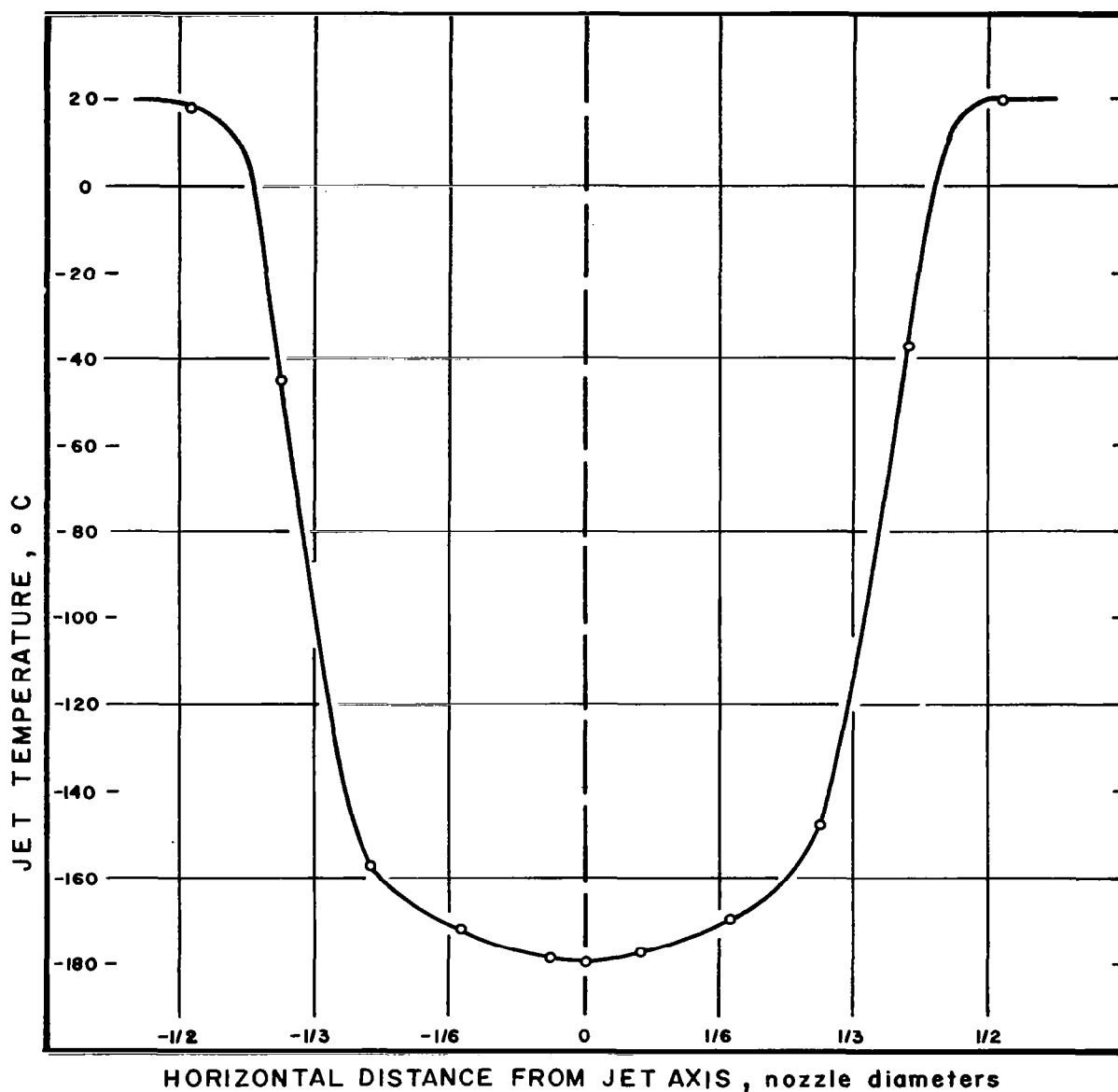


FIG.3. LOW TEMP. NITROGEN JET FACILITY



**FIG.4. HORIZONTAL TEMPERATURE TRAVERSE  
3/4" (I D) FROM NOZZLE ; M = 0.078**

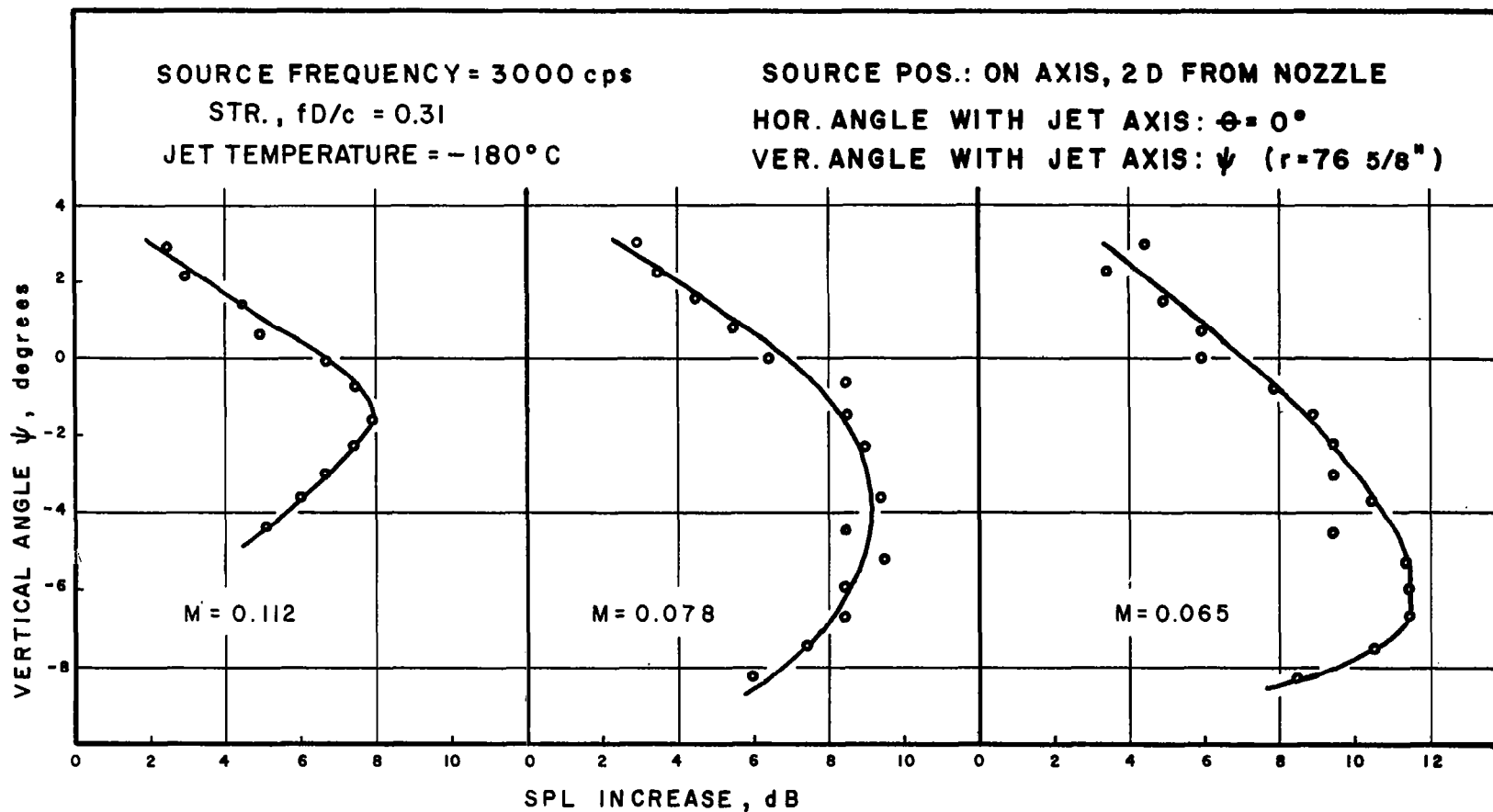
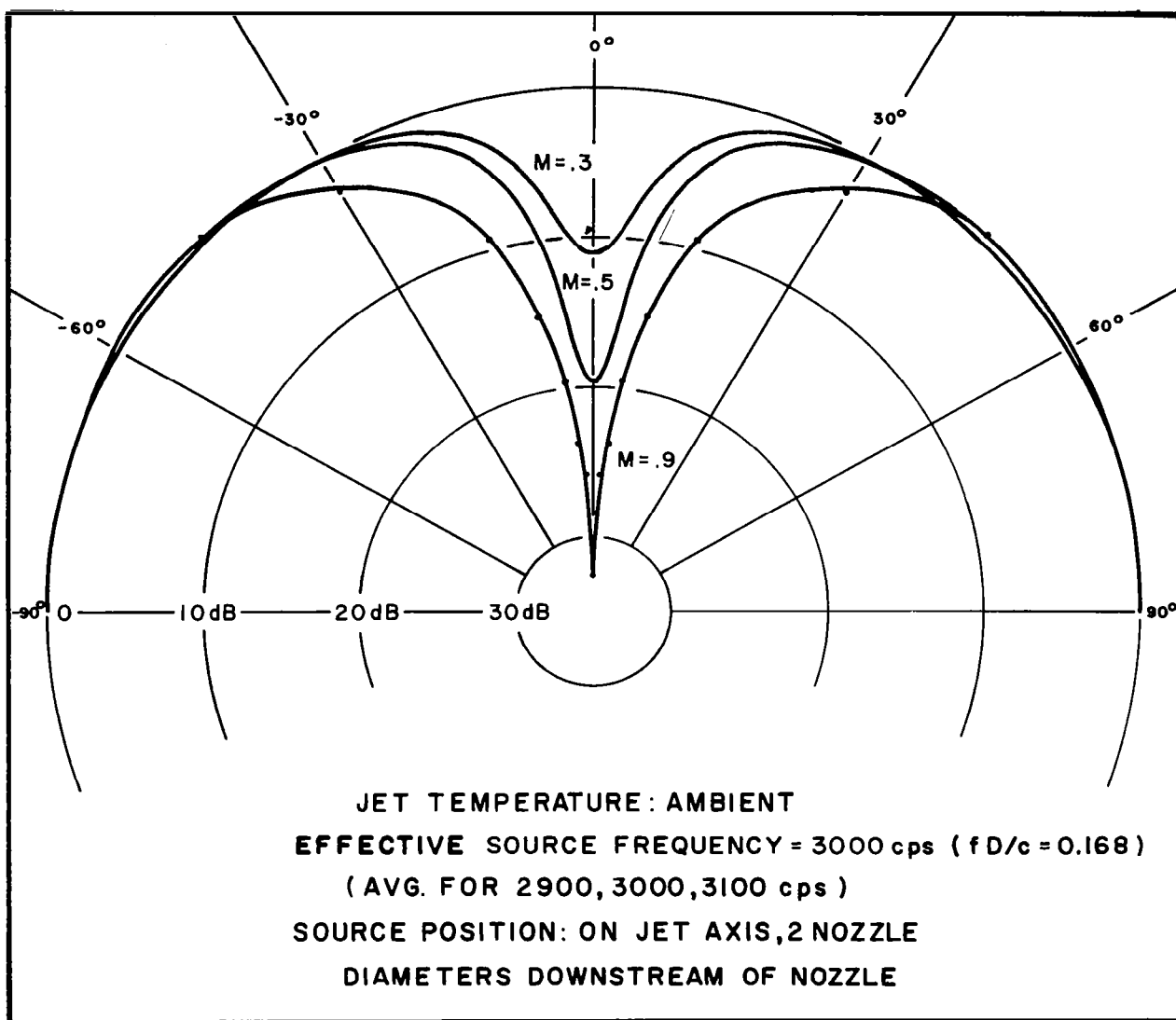


FIG.5. VELOCITY DEPENDENCE OF DROOP OF JET



**FIG.6. EFFECT OF JET VELOCITY ON DIRECTIVITY**

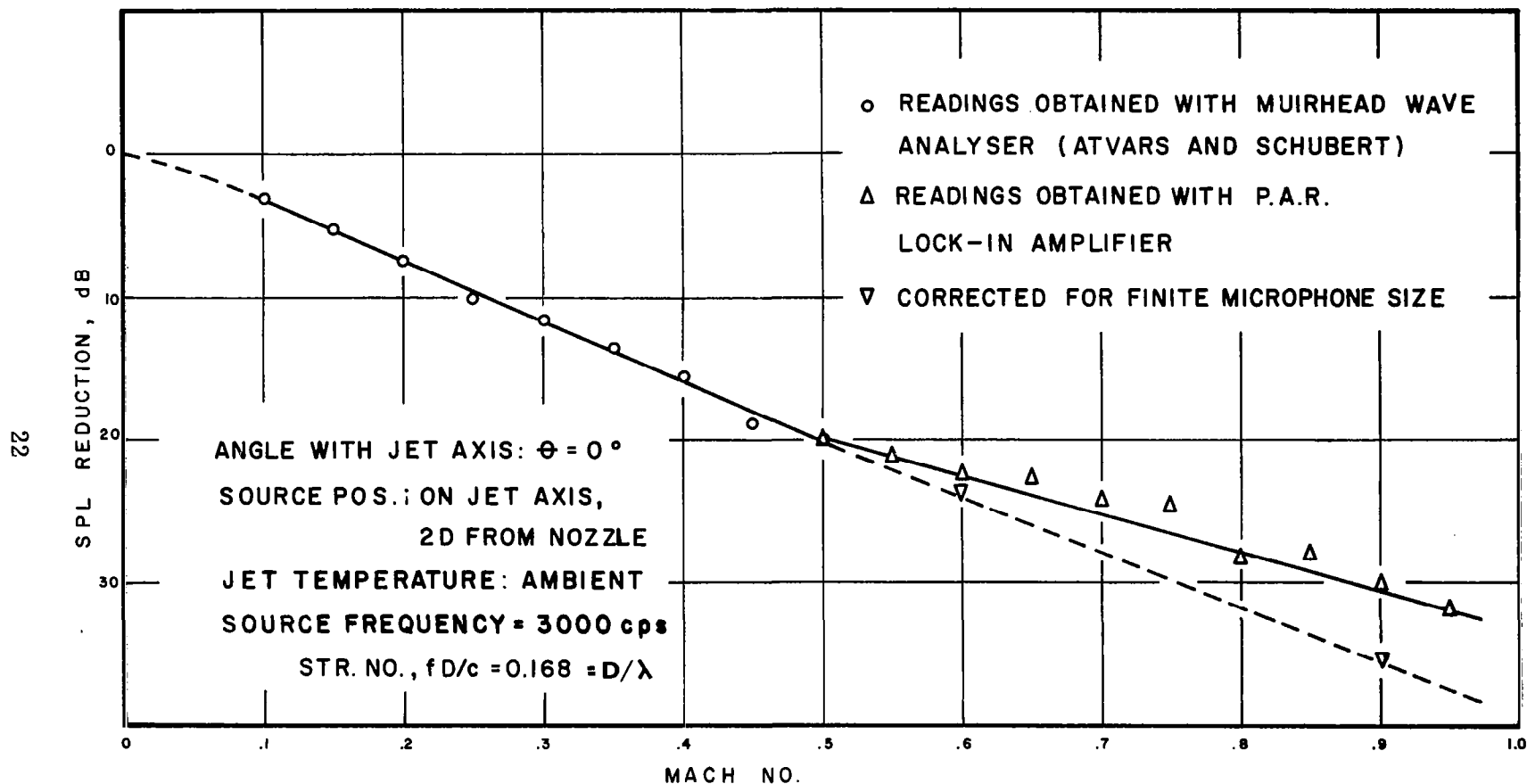


FIG. 7. VELOCITY DEPENDENCE OF REFRACTION

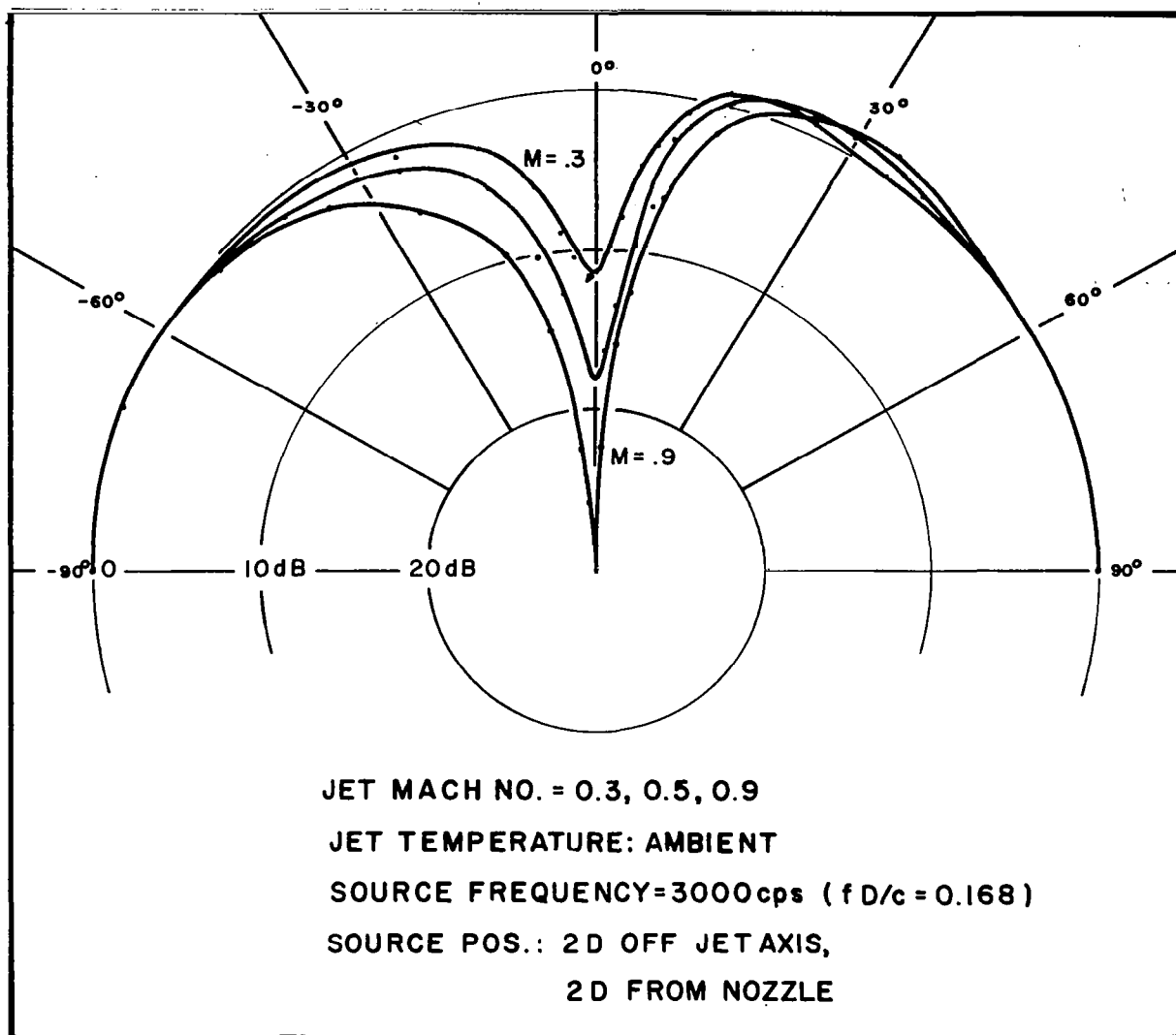


FIG. 8

## EFFECT OF JET VELOCITY ON DIRECTIVITY FOR OFF-AXIS SOURCE POSITION

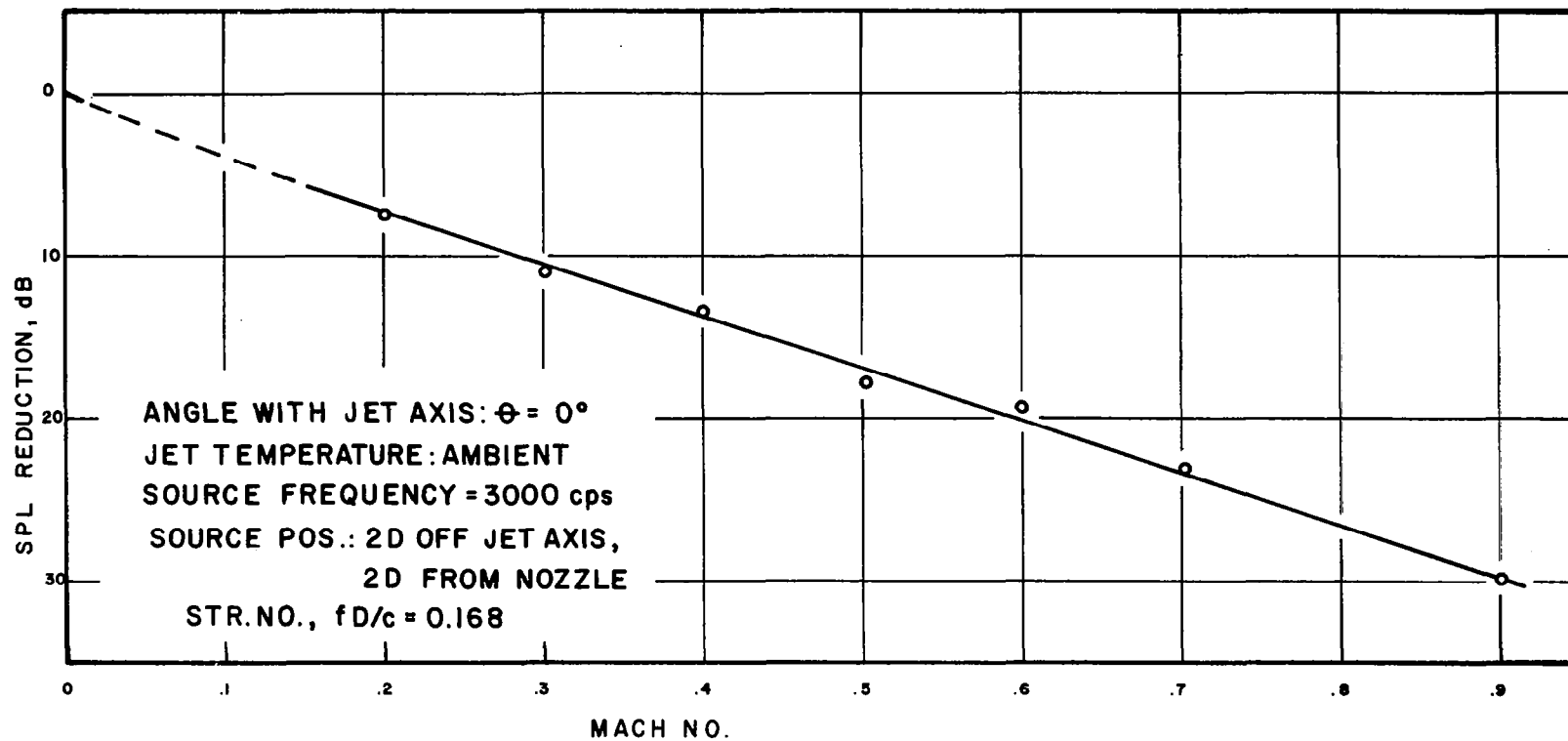


FIG.9. VELOCITY DEPENDENCE OF REFRACTION  
FOR OFF-AXIS SOURCE POSITION



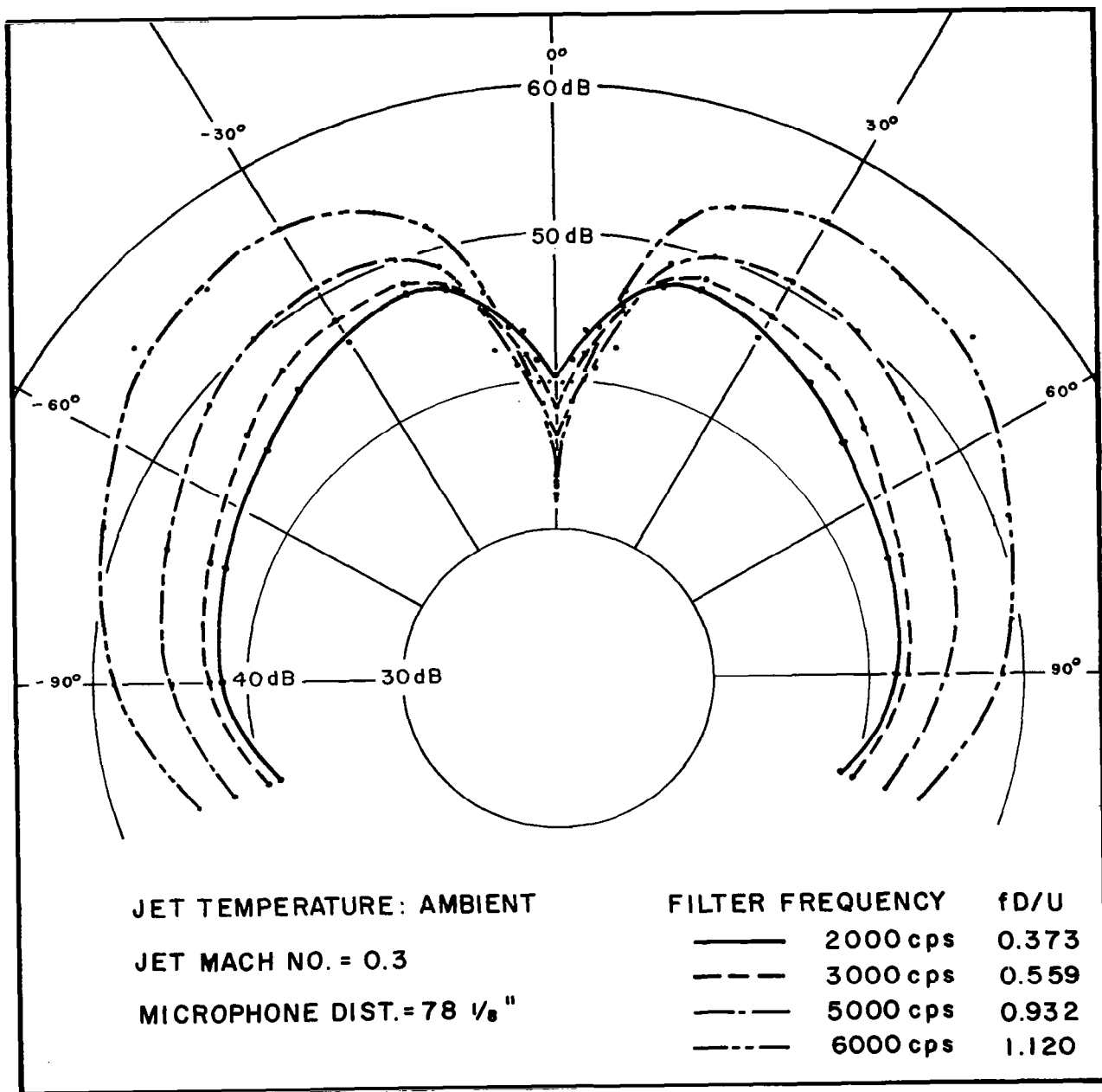


FIG.10. JET NOISE DIRECTIVITY FOR AIR JET

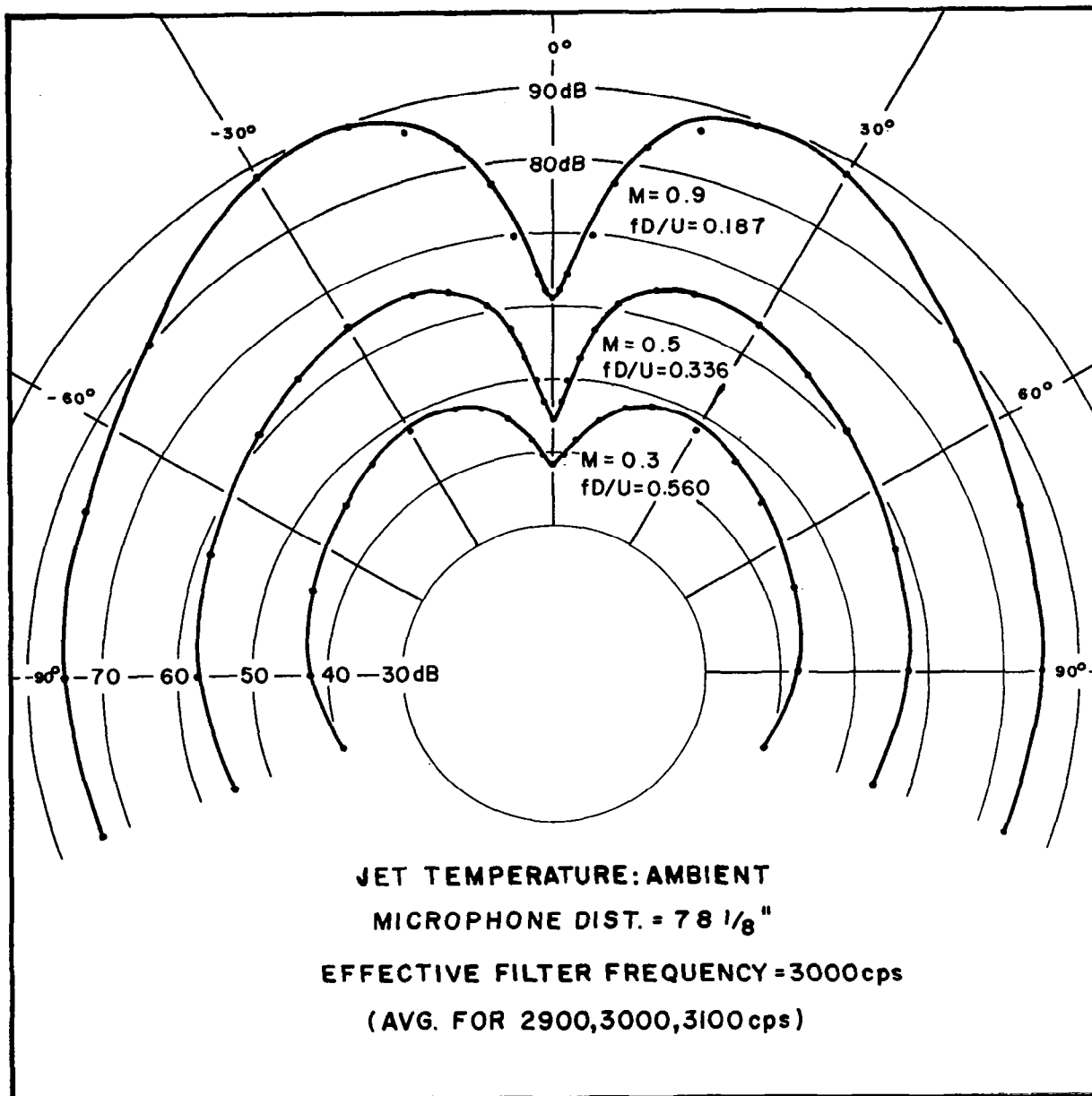


FIG.II. JET NOISE DIRECTIVITY FOR AIR JET

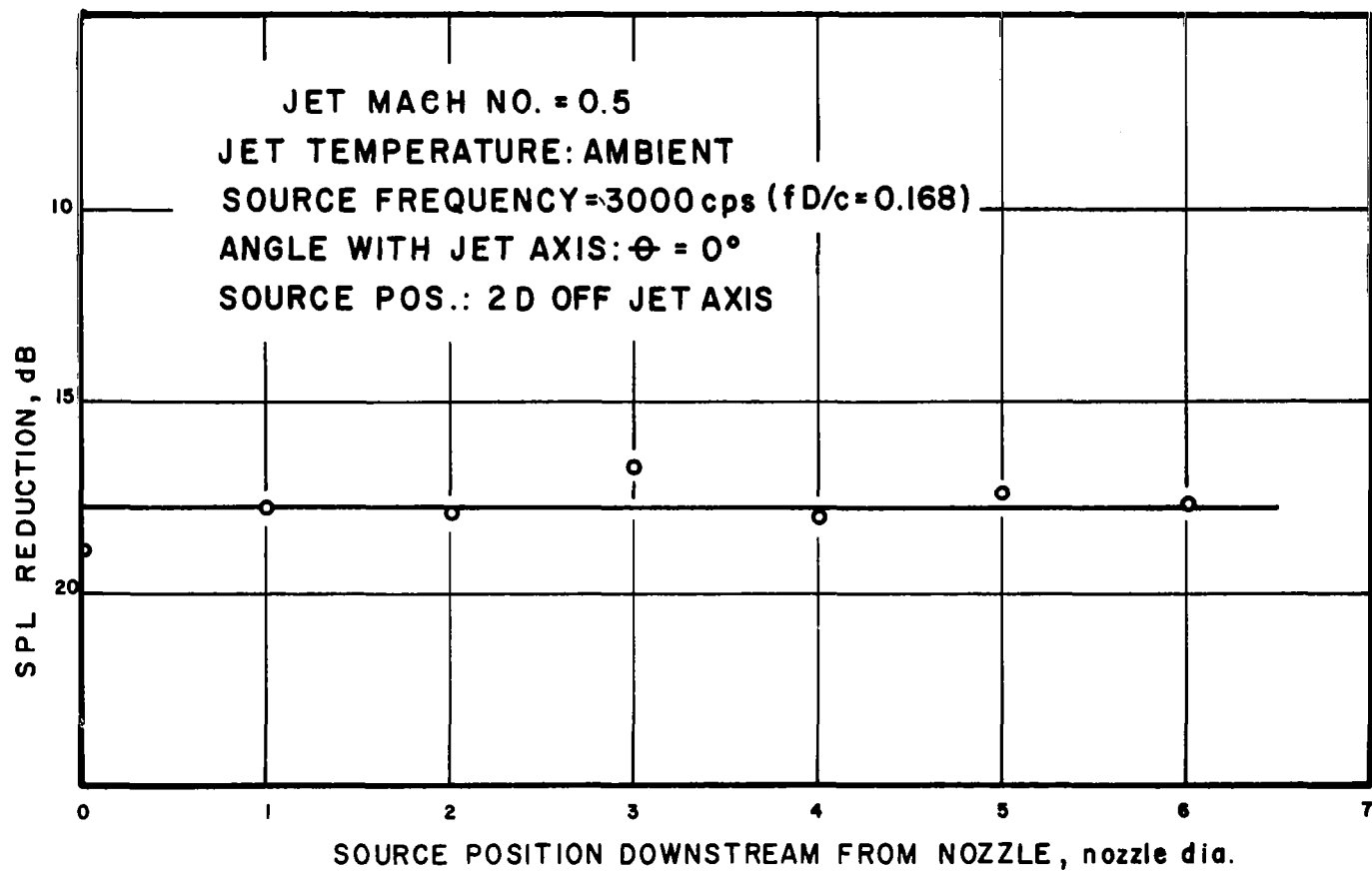


FIG.12. EFFECT OF SOURCE POS. ON REFRACTION

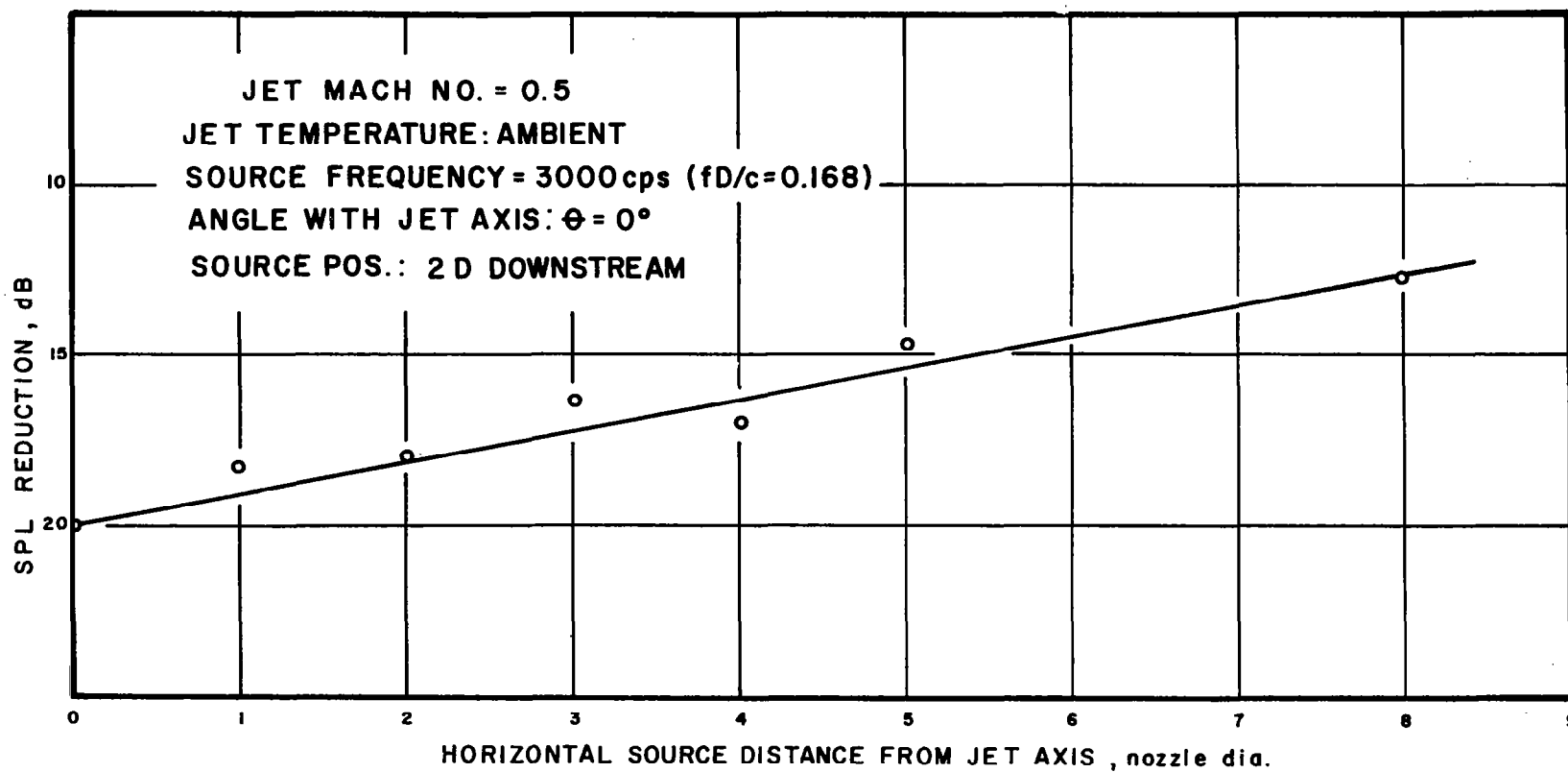
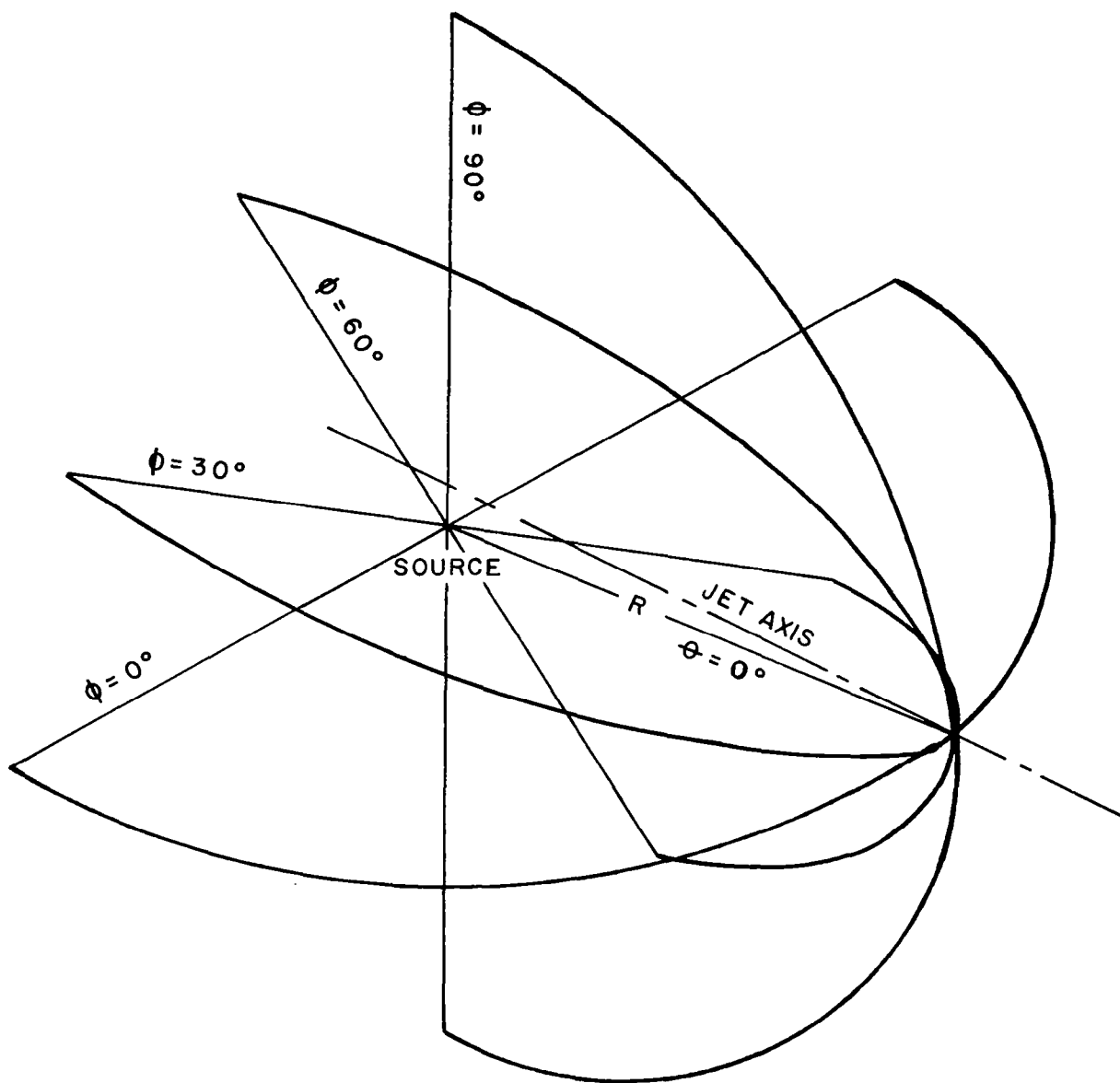


FIG.13. EFFECT OF SOURCE POSITION ON REFRACTION



SOURCE — MICROPHONE DIST. :  $R = 76 \frac{5}{8}''$

MICROPHONE TRAVERSES CROSS

JET AXIS AT  $\theta = 0^\circ$

FIG.14. MICROPHONE TRAVERSES FOR  
OFF-AXIS SOURCE POSITIONS

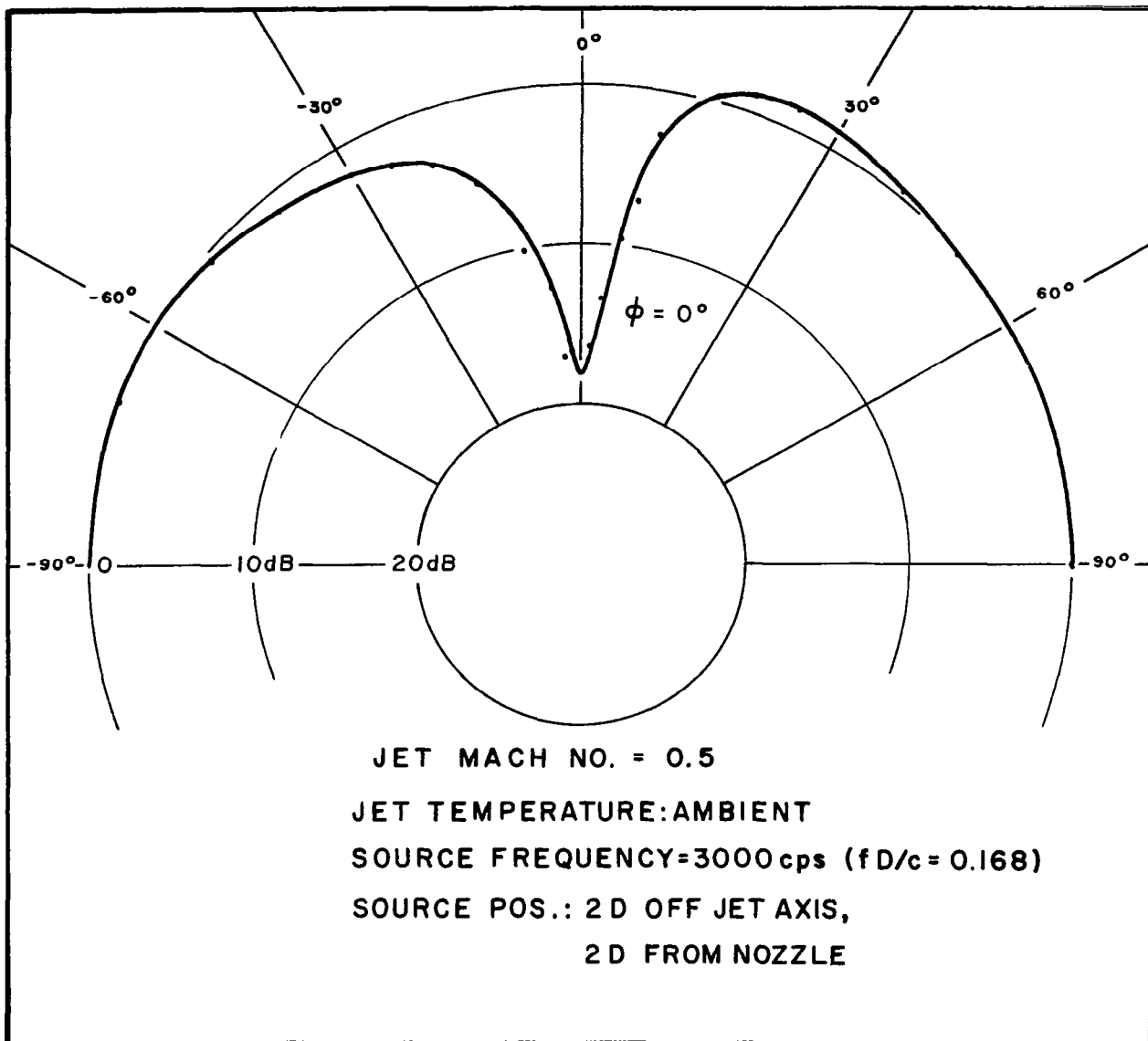


FIG. 15. DIRECTIVITY PATTERN FOR  $\phi = 0^\circ$

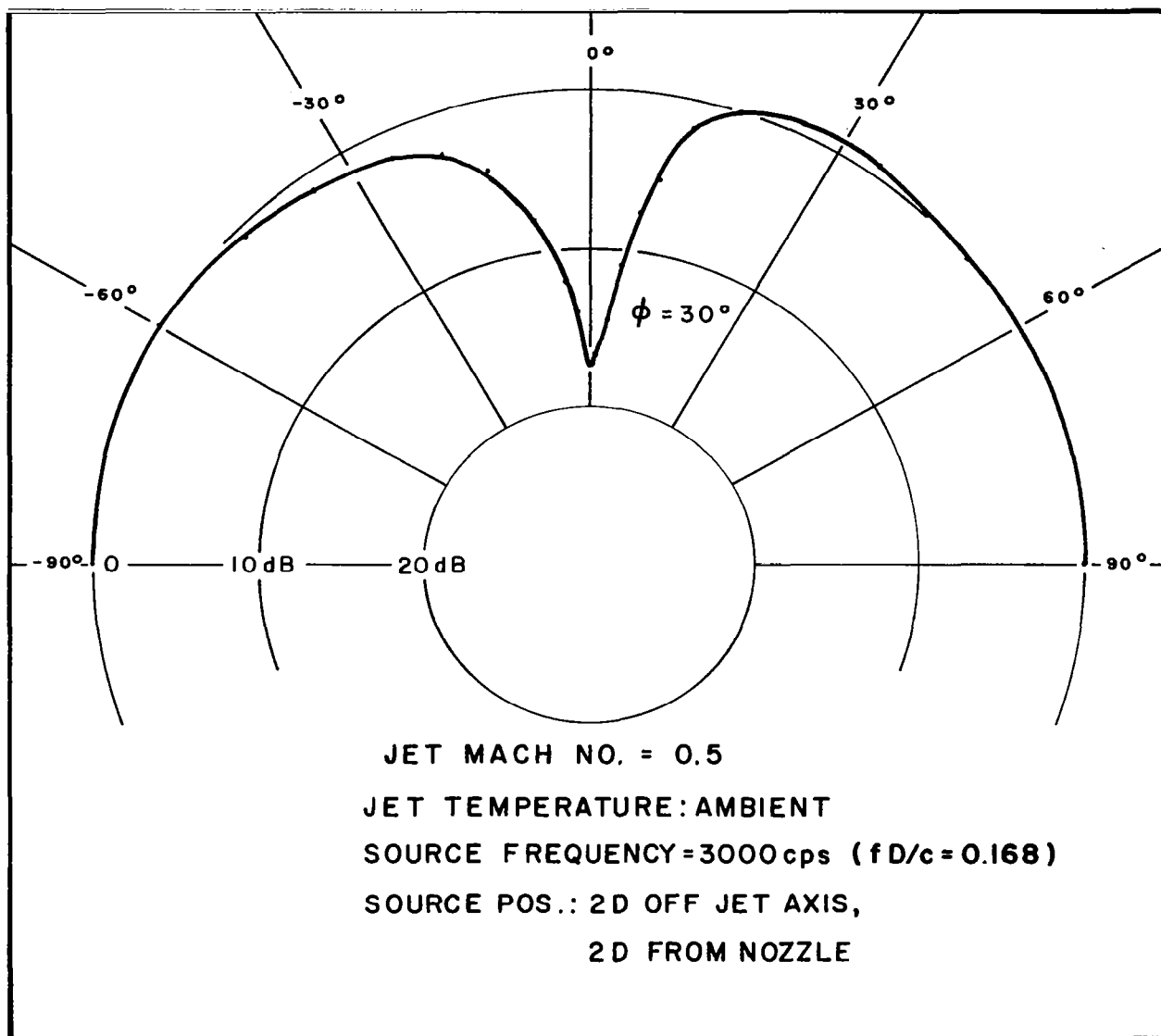


FIG. 16. DIRECTIVITY PATTERN FOR  $\Phi = 30^\circ$

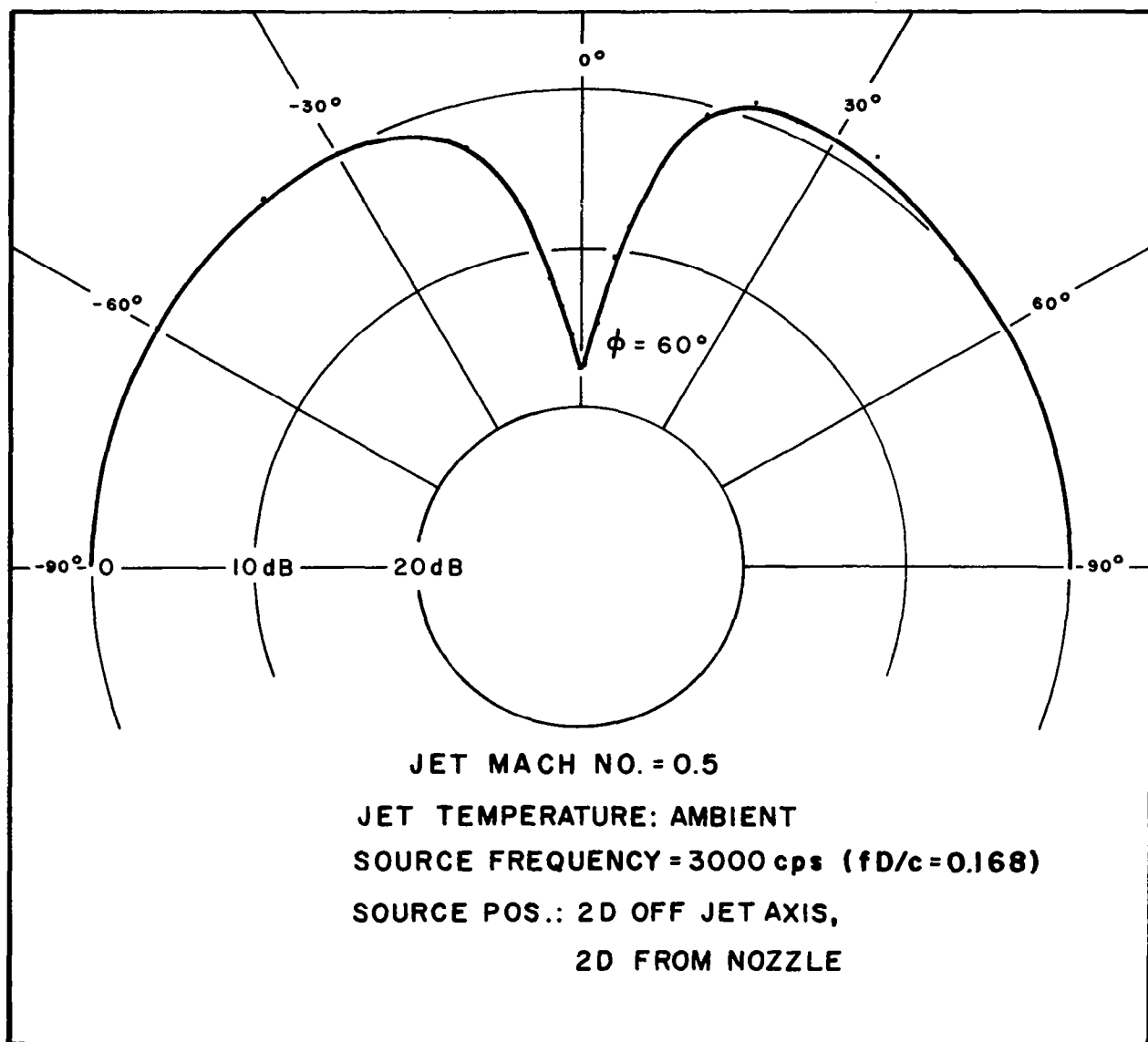


FIG.17. DIRECTIVITY PATTERN FOR  $\Phi = 60^\circ$



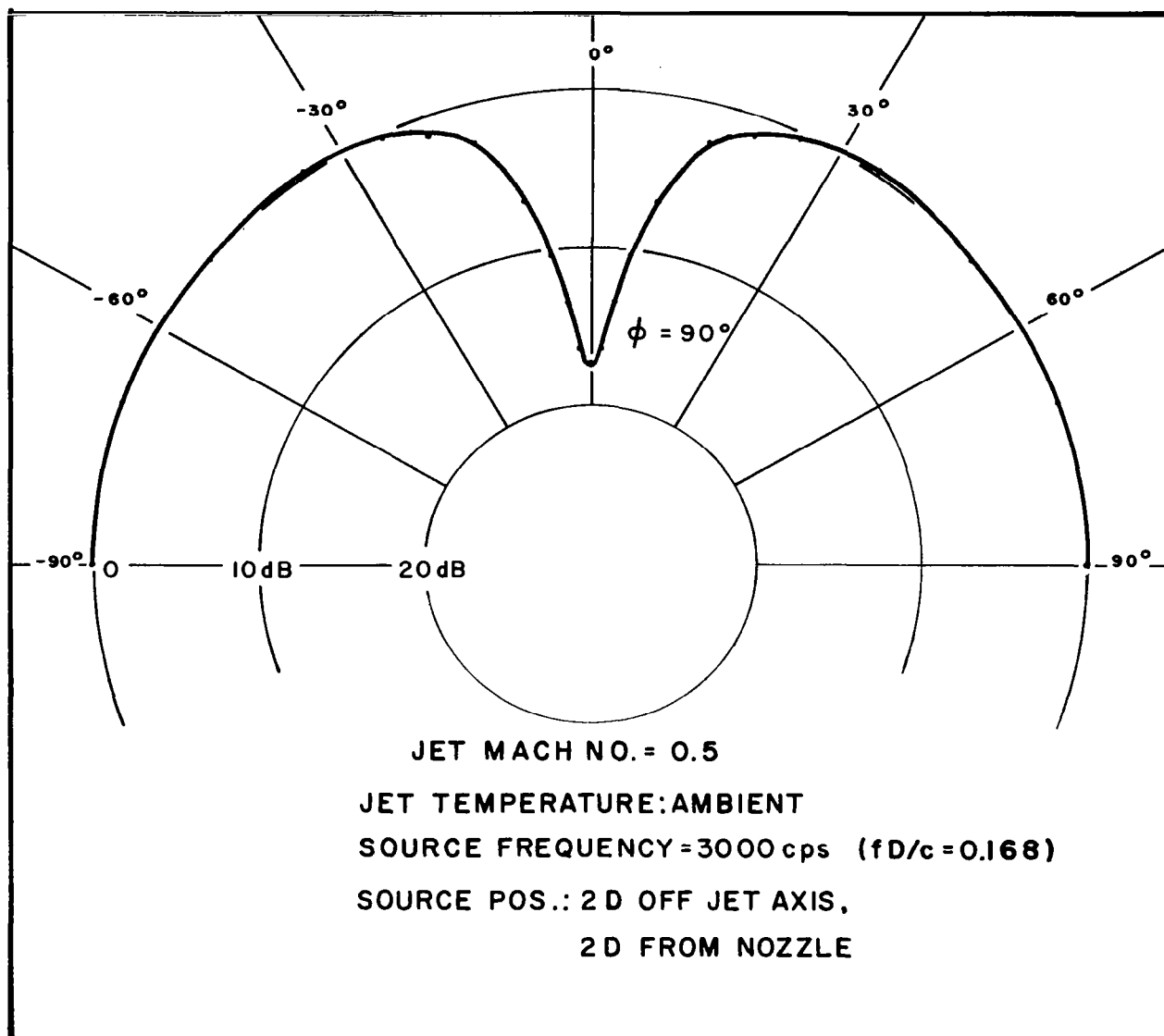


FIG. 18. DIRECTIVITY PATTERN FOR  $\Phi = 90^\circ$

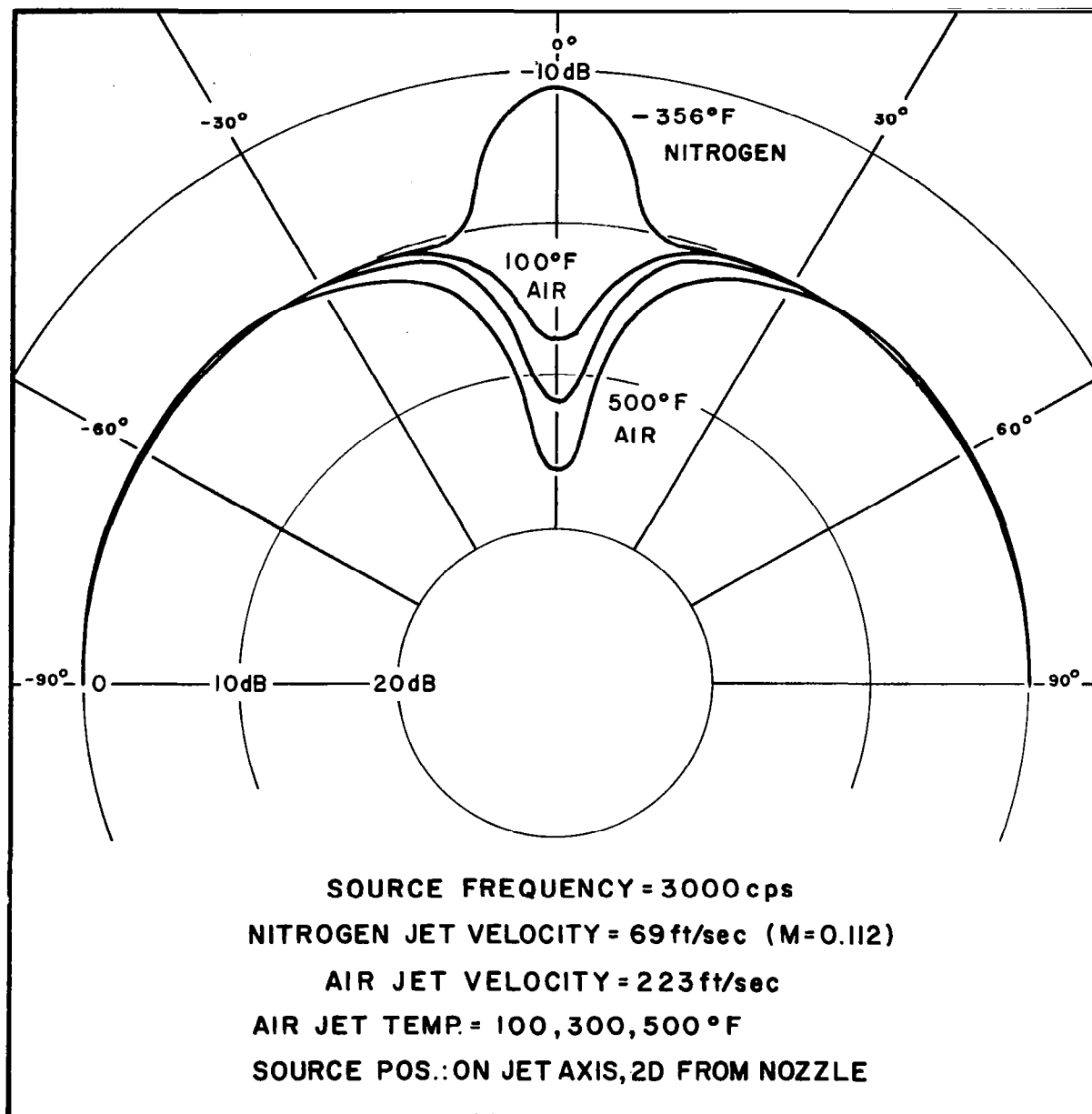


FIG. 19

## EFFECT OF JET TEMPERATURE ON DIRECTIVITY

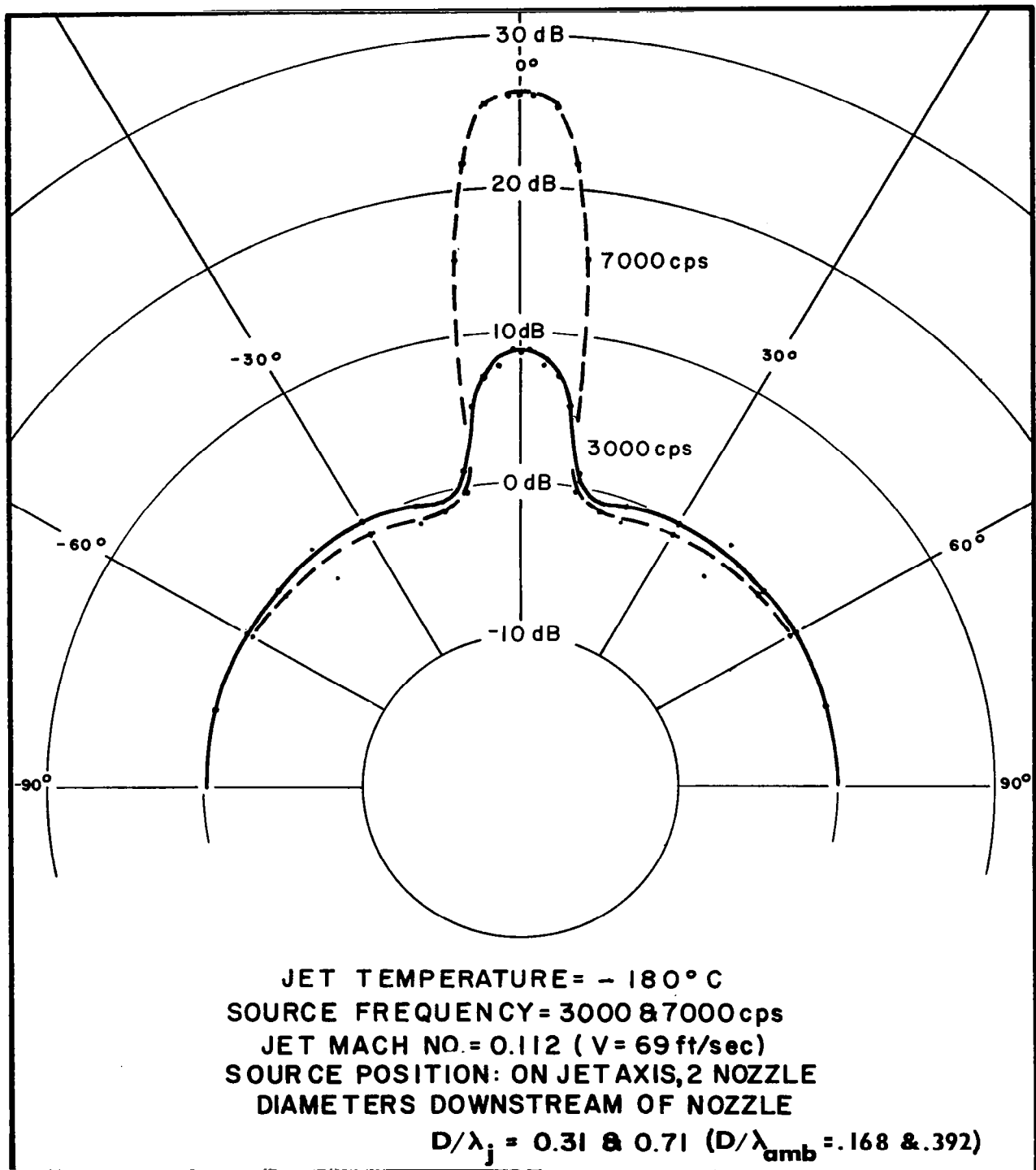


FIG.20.EFFECT OF SOURCE FREQUENCY ON  
DIRECTIVITY OF NITROGEN JET

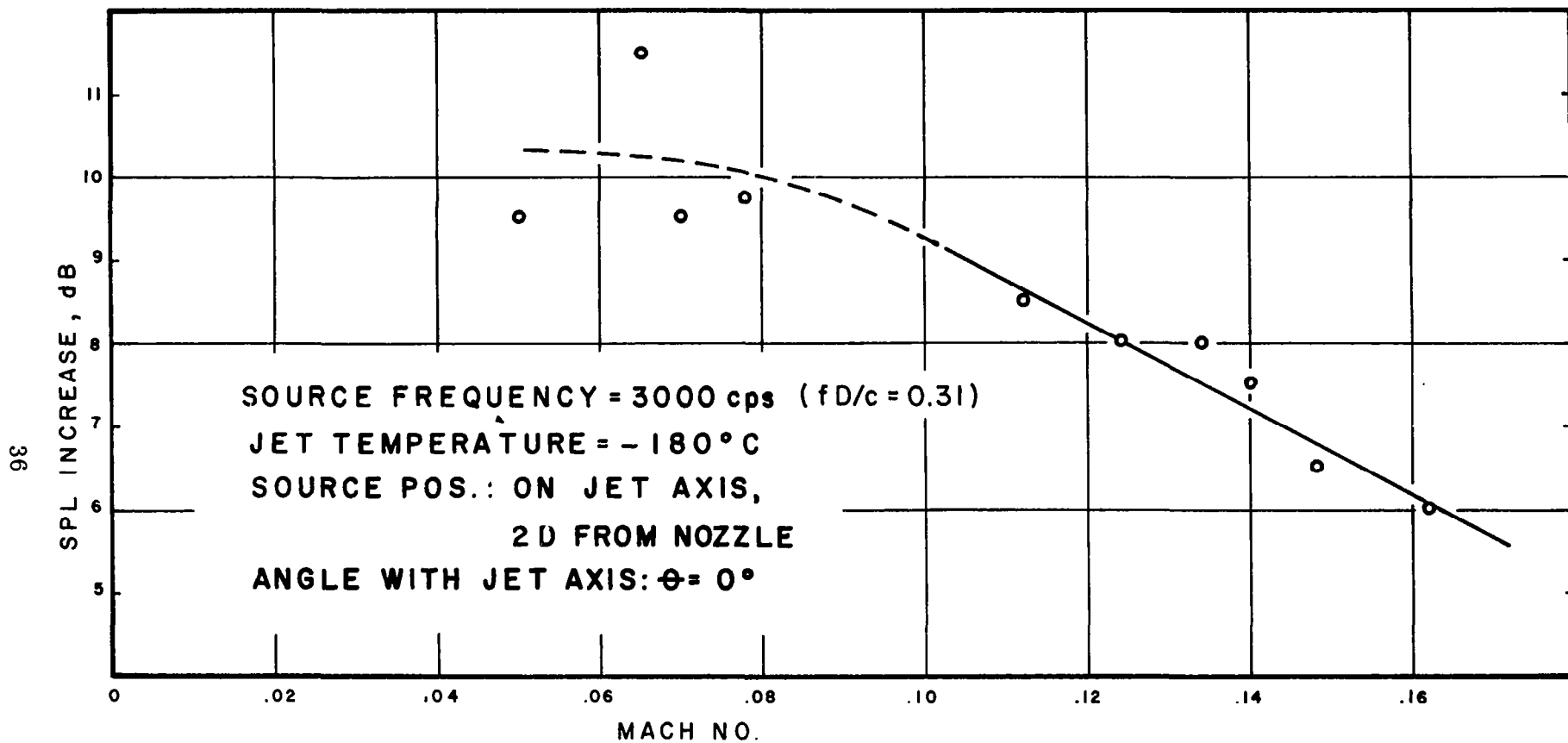


FIG.21. VELOCITY DEPENDENCE OF REFRACTION  
FOR NITROGEN JET

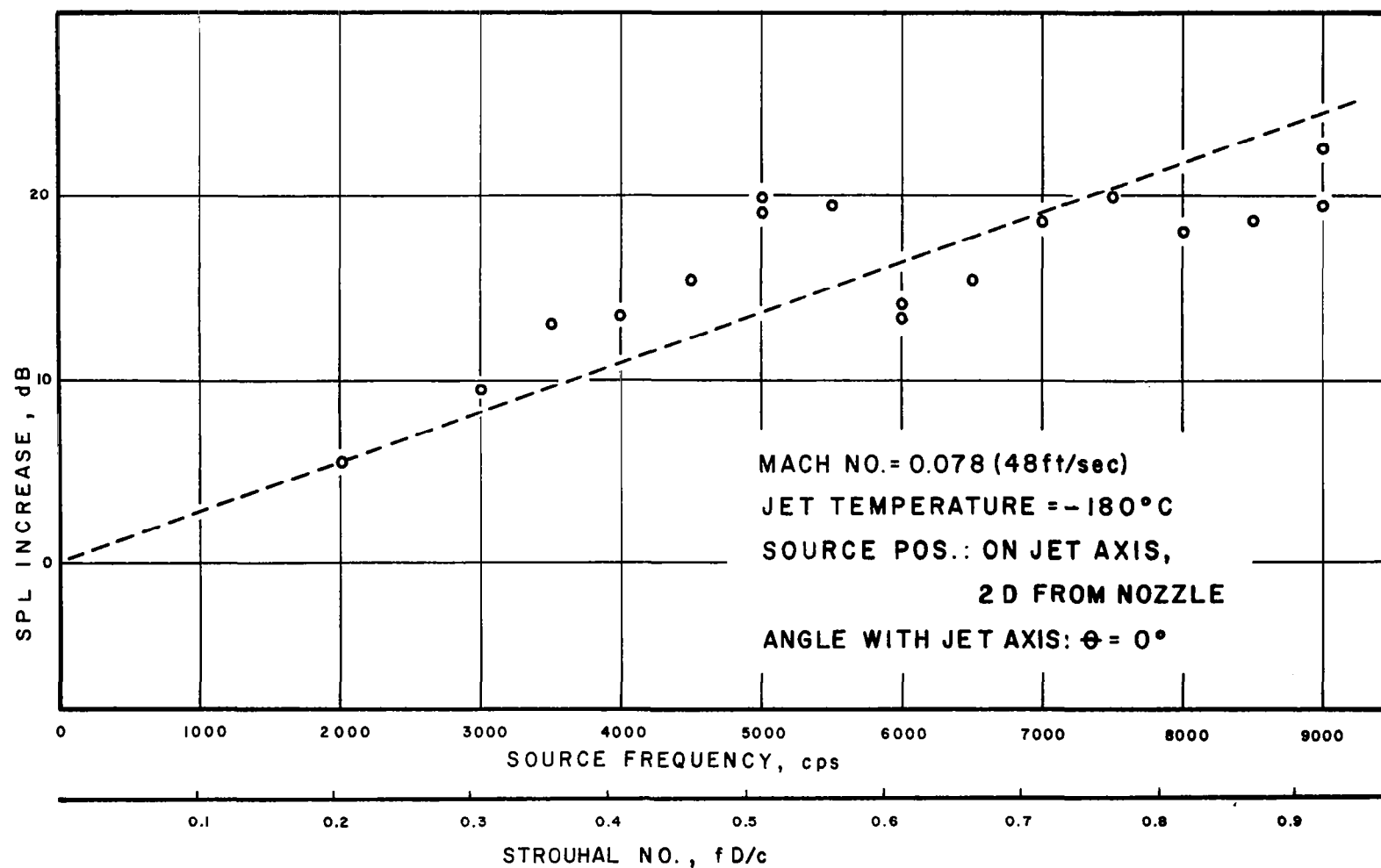


FIG.22.FREQUENCY DEPENDENCE OF REFRACTION  
FOR NITROGEN JET

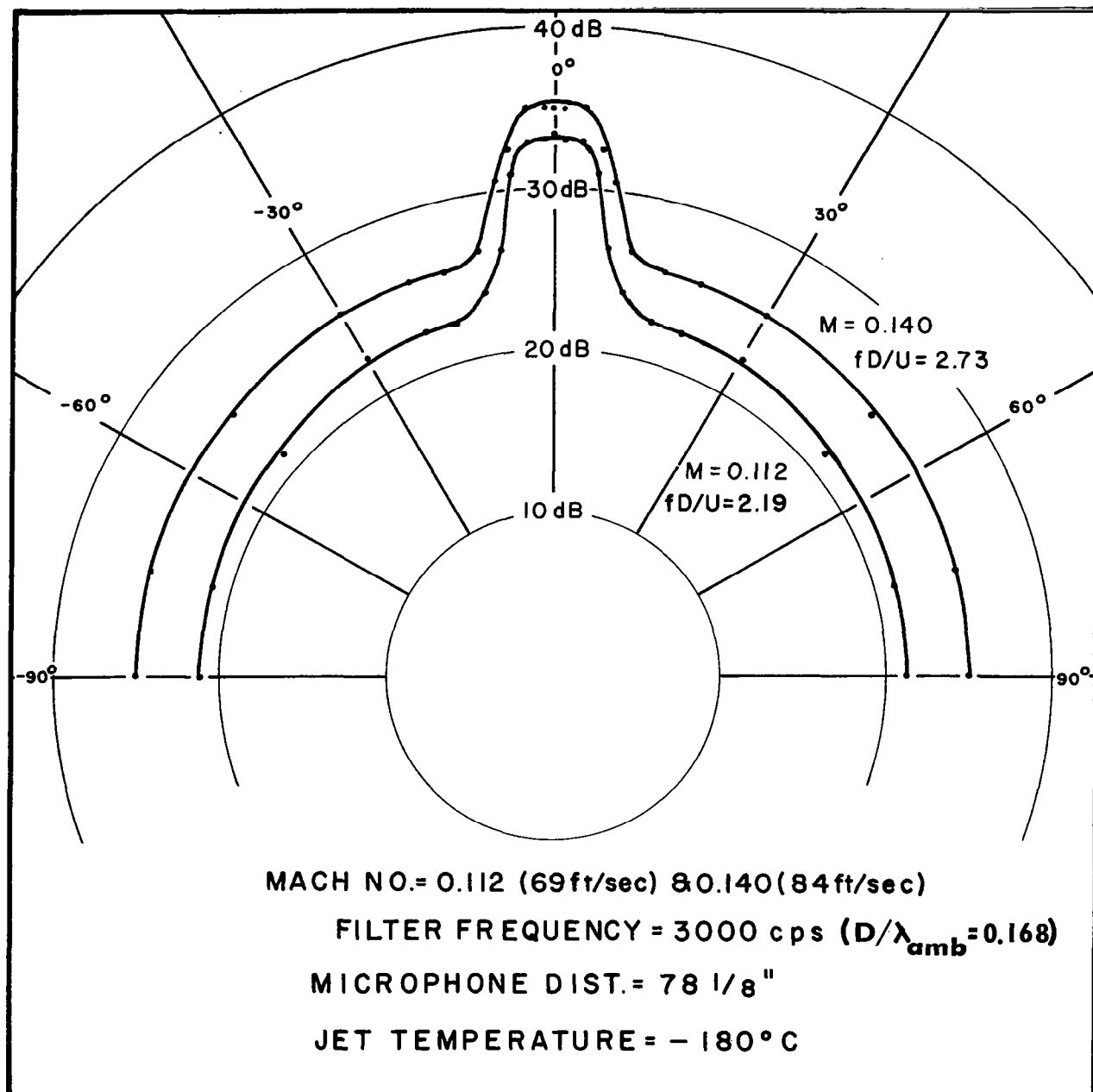
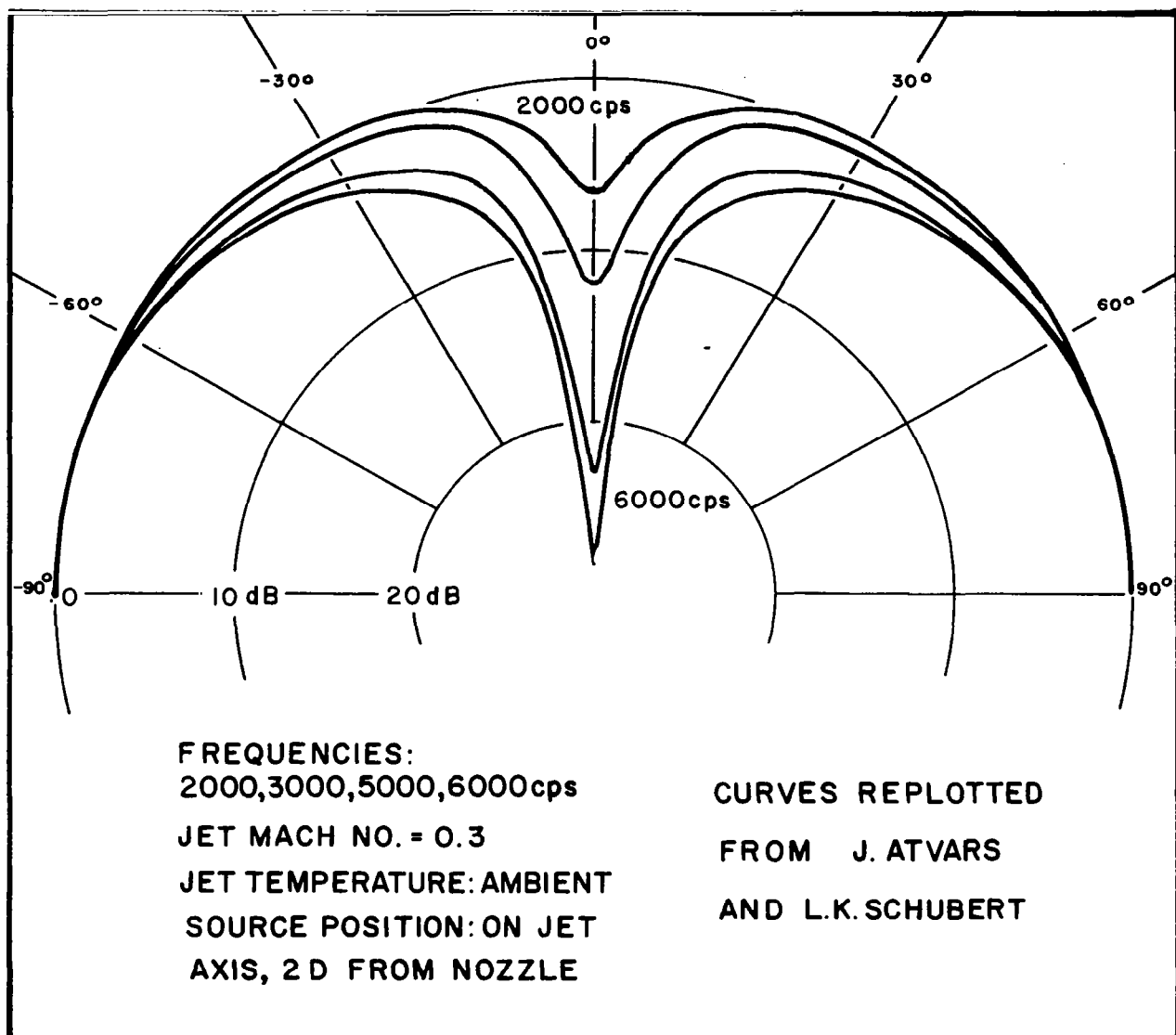


FIG.23. JET NOISE DIRECTIVITY FOR  
 3/4" NITROGEN JET



**FIG.24.EFFECT OF SOURCE FREQUENCY  
ON DIRECTIVITY**

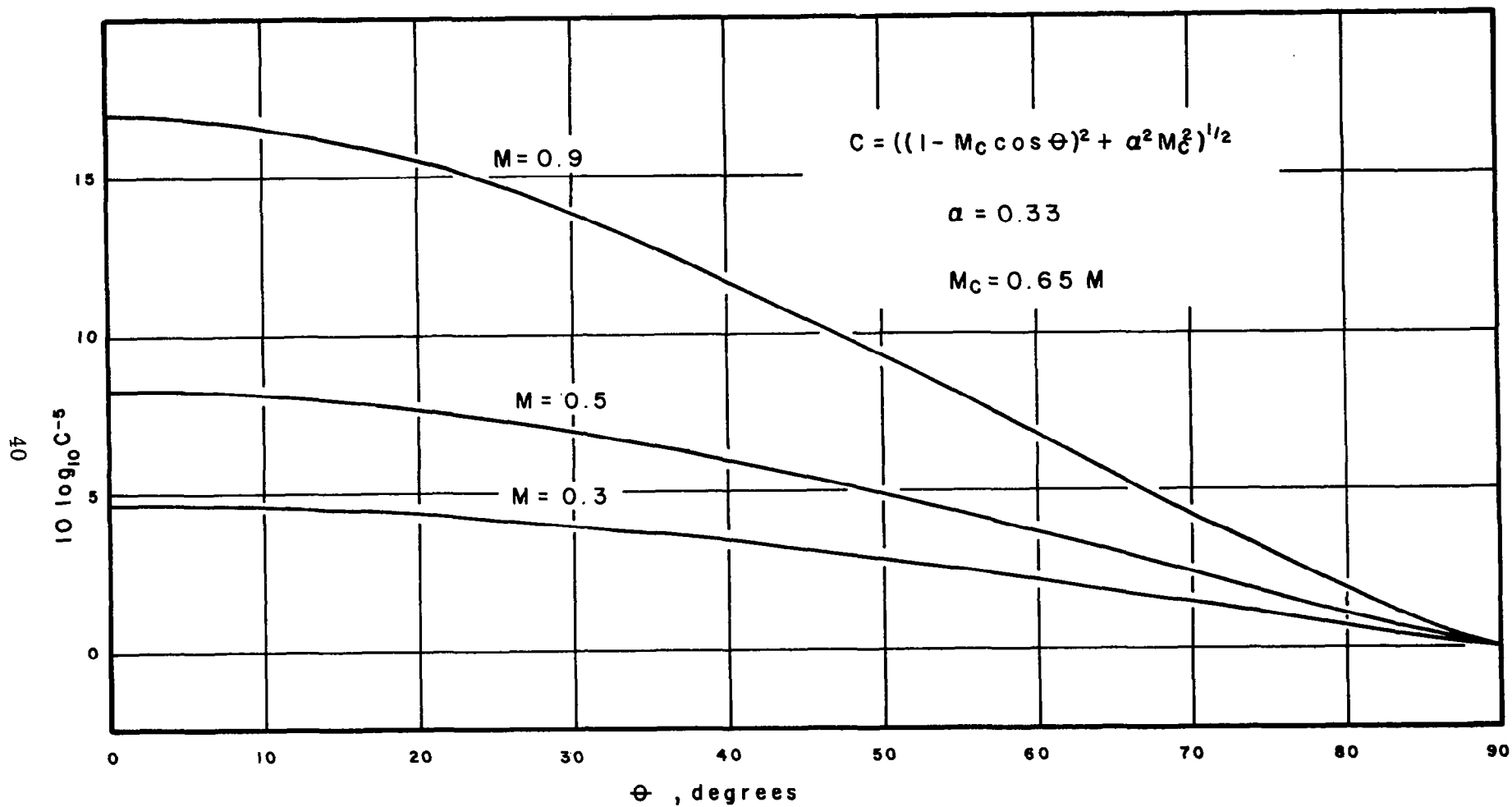


FIG.25. CONVECTION DIRECTIVITY FACTOR



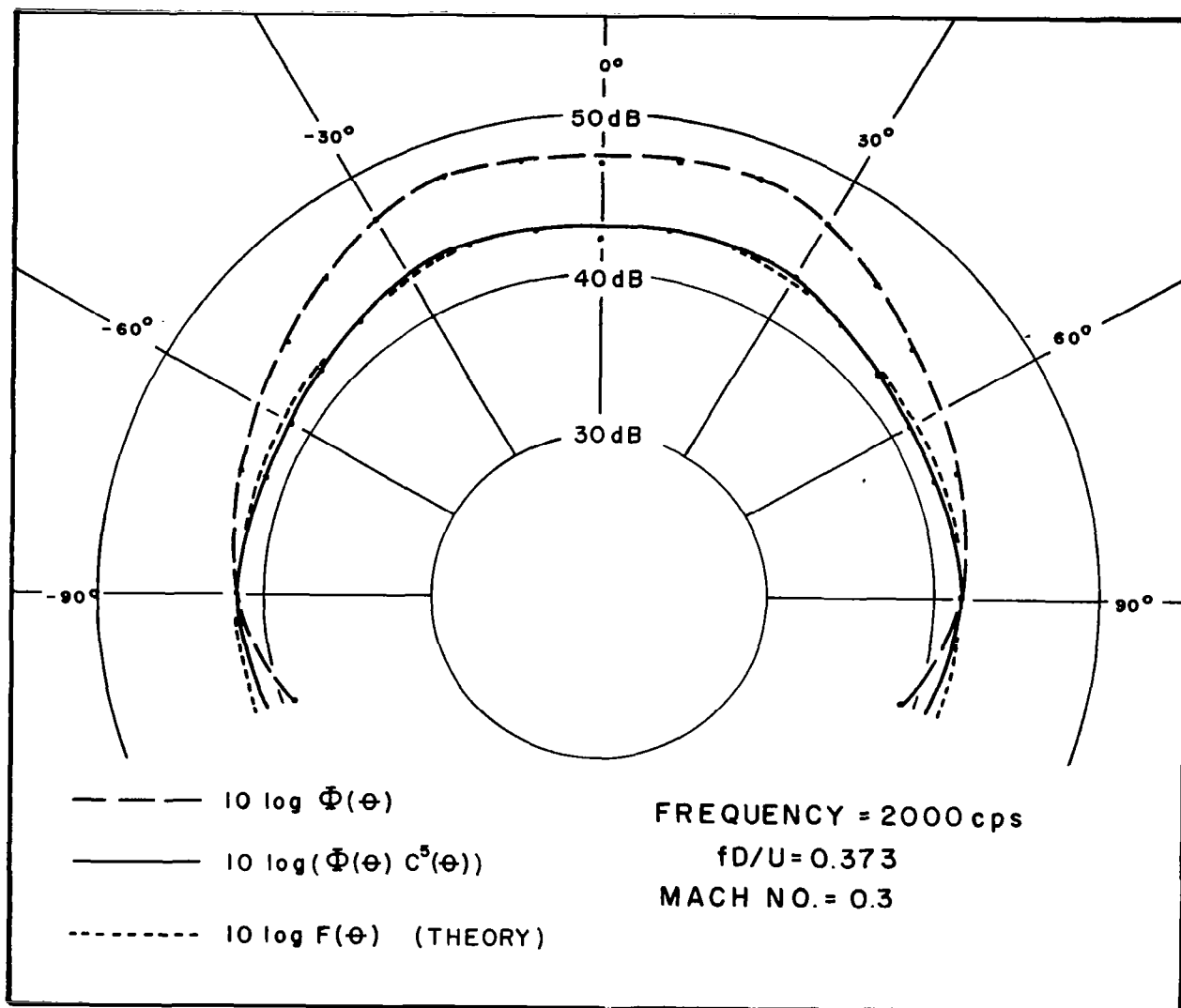


FIG.26. COMPARISON OF EXPERIMENTAL AND THEORETICAL BASIC DIRECTIVITY

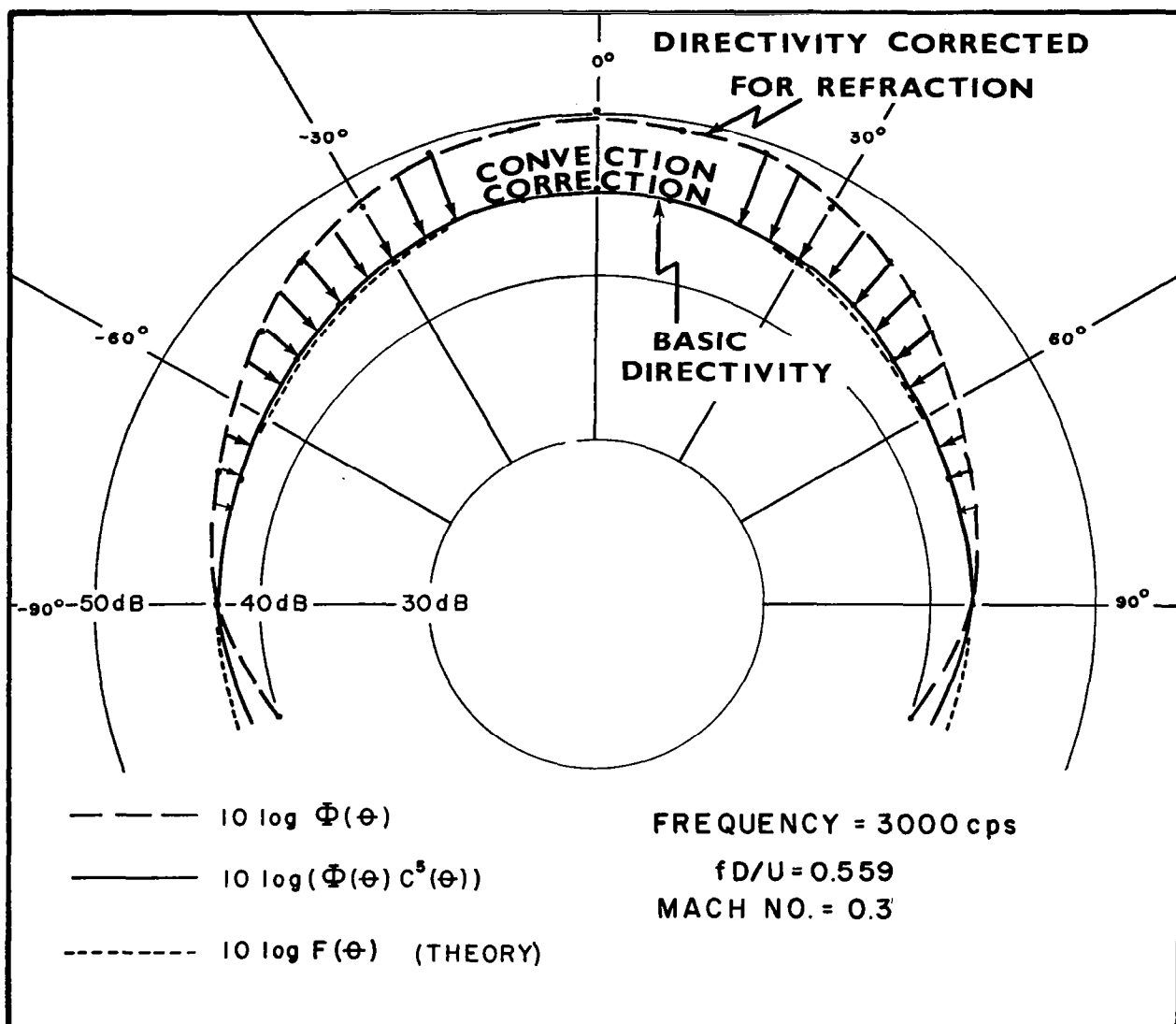


FIG.27. COMPARISON OF EXPERIMENTAL AND THEORETICAL BASIC DIRECTIVITY

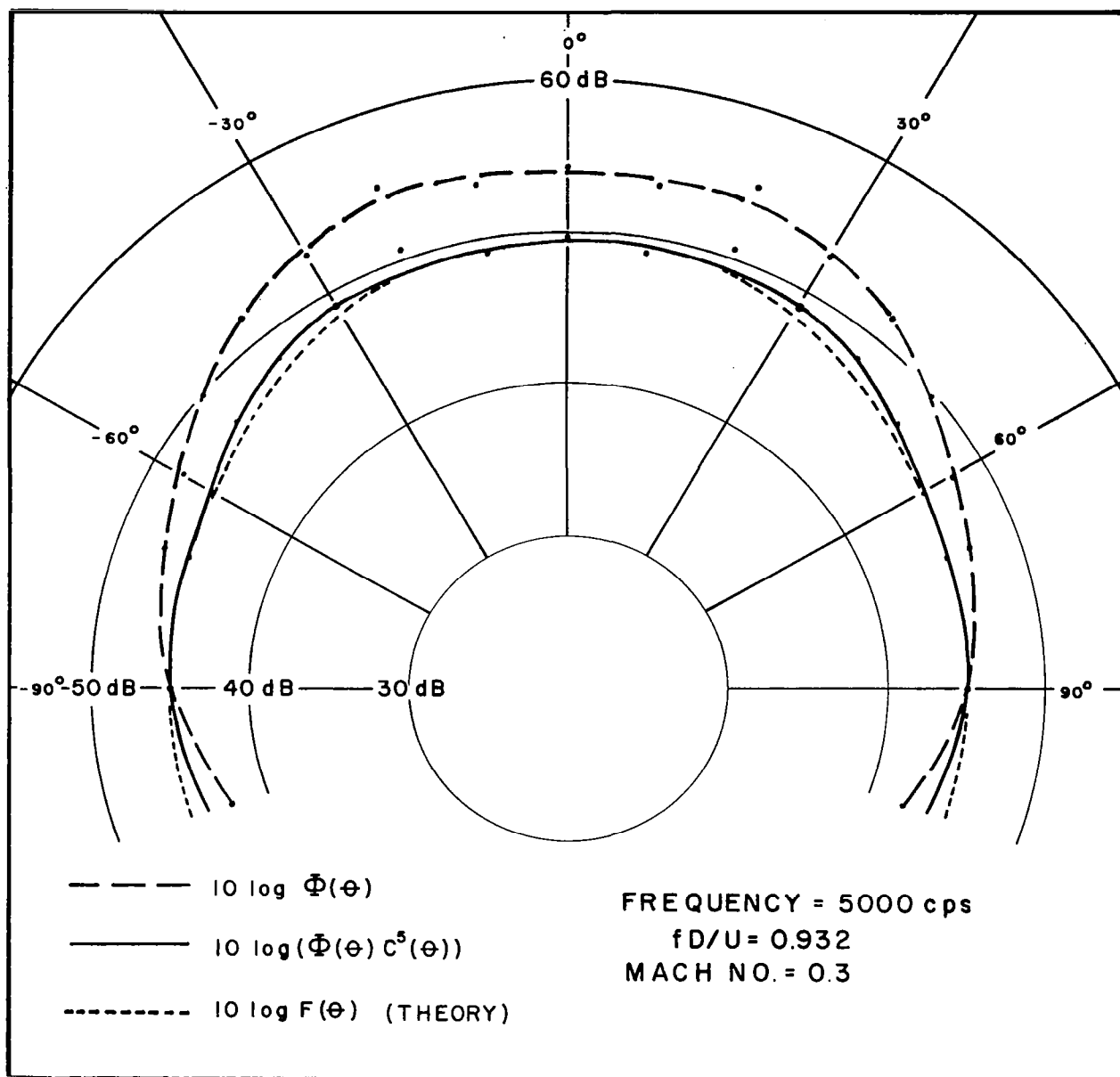


FIG.28. COMPARISON OF EXPERIMENTAL AND THEORETICAL BASIC DIRECTIVITY

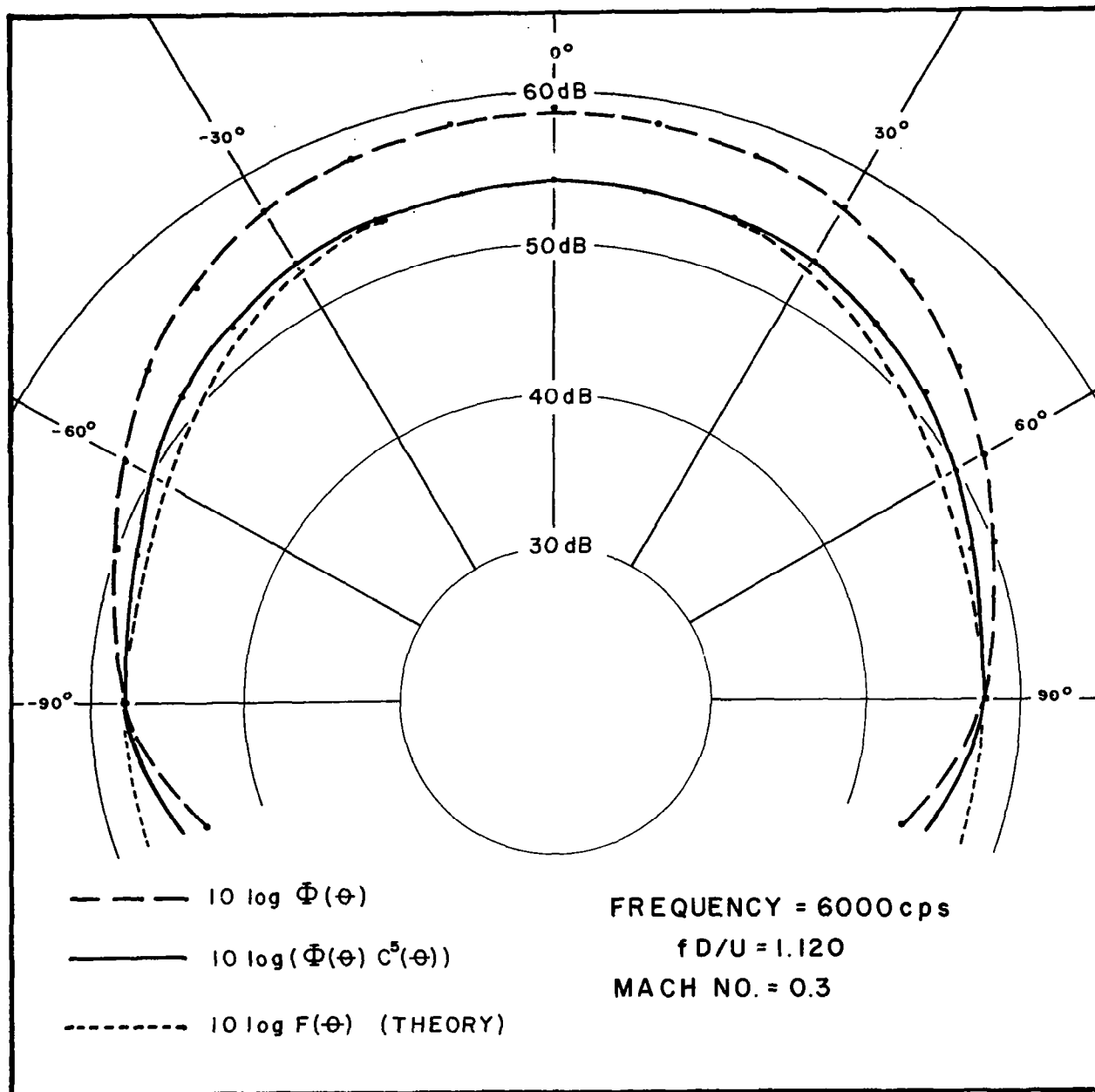


FIG.29. COMPARISON OF EXPERIMENTAL AND THEORETICAL BASIC DIRECTIVITY

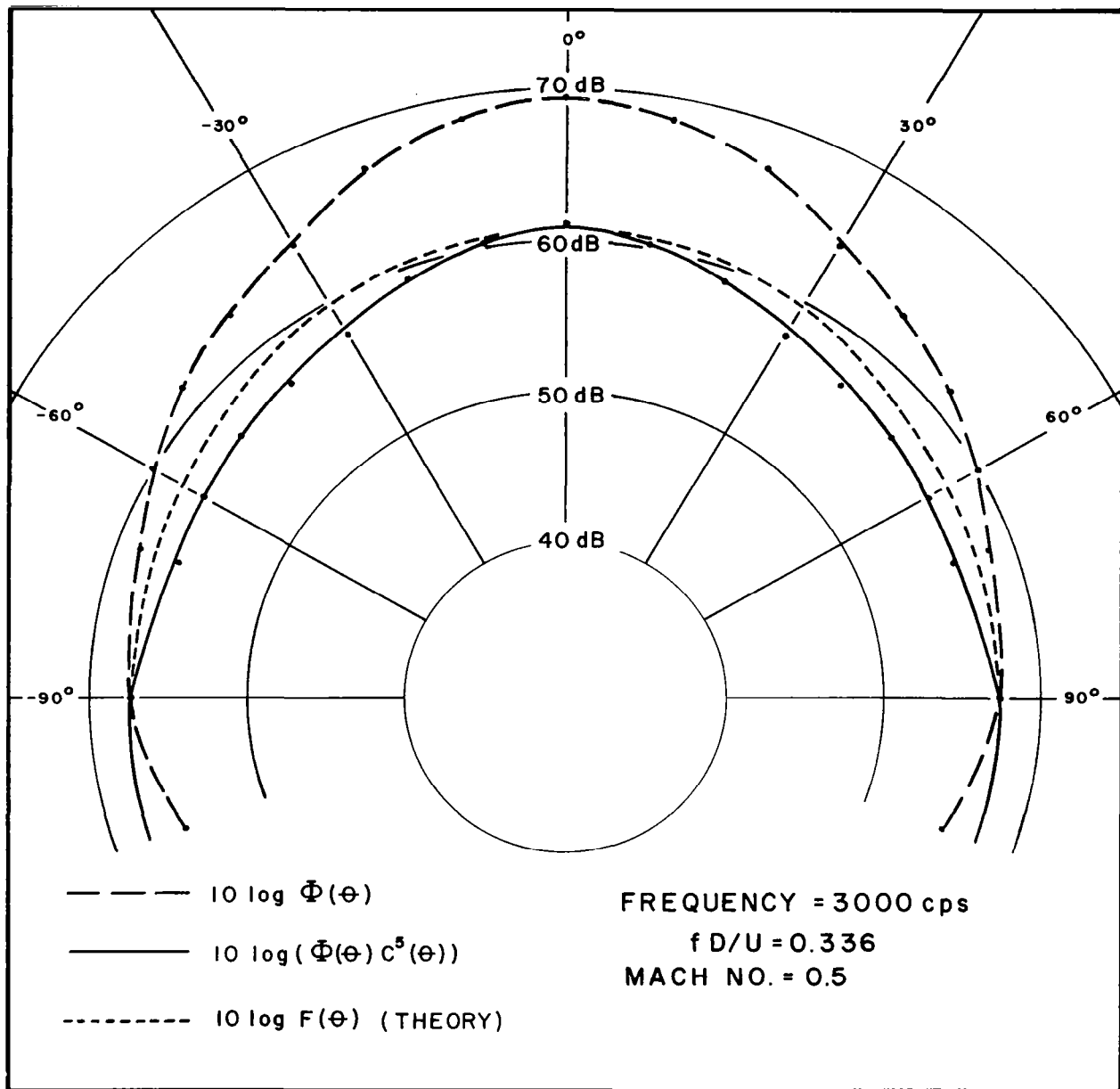


FIG.30. COMPARISON OF EXPERIMENTAL AND THEORETICAL BASIC DIRECTIVITY

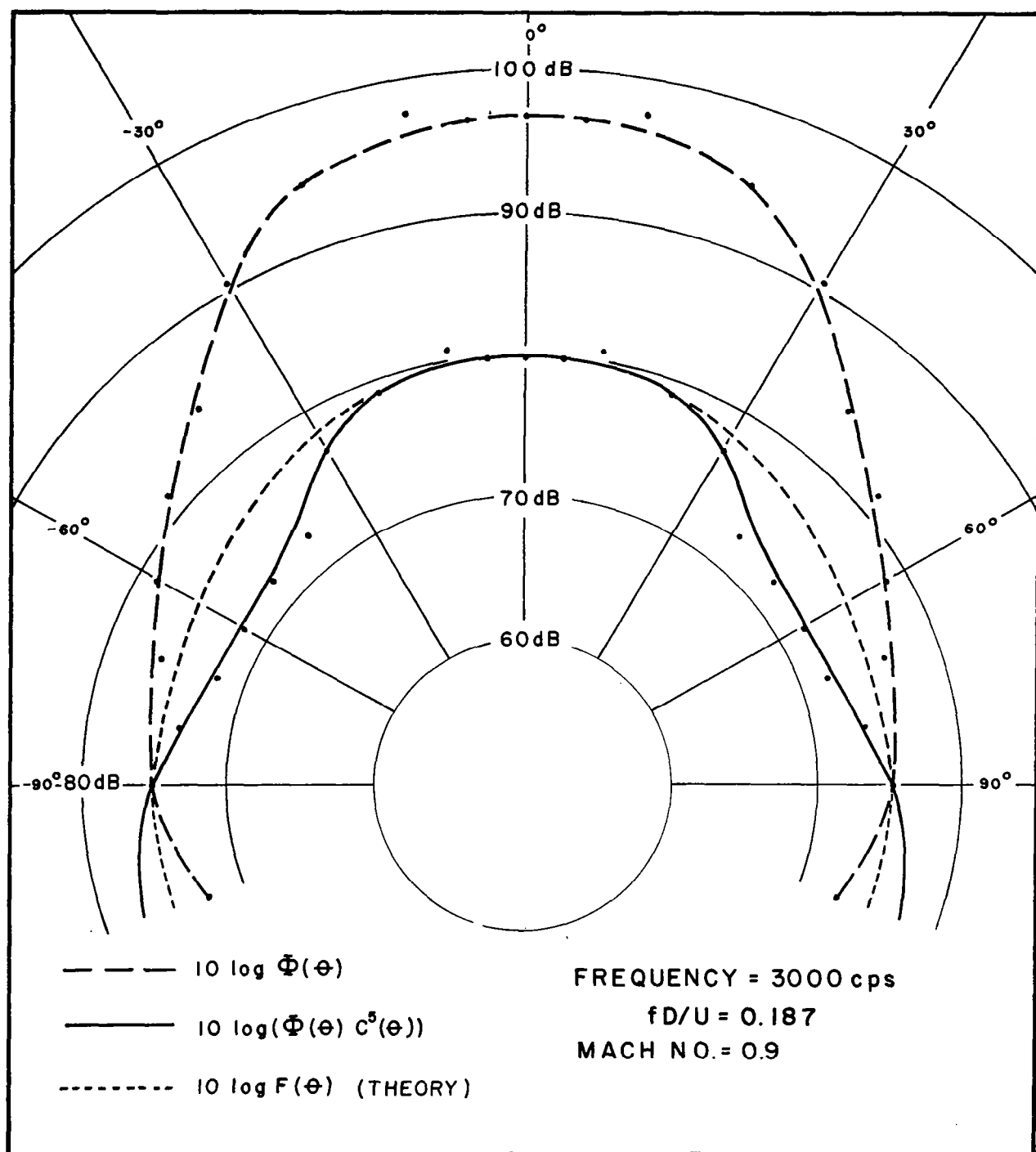


FIG.31. COMPARISON OF EXPERIMENTAL AND THEORETICAL BASIC DIRECTIVITY

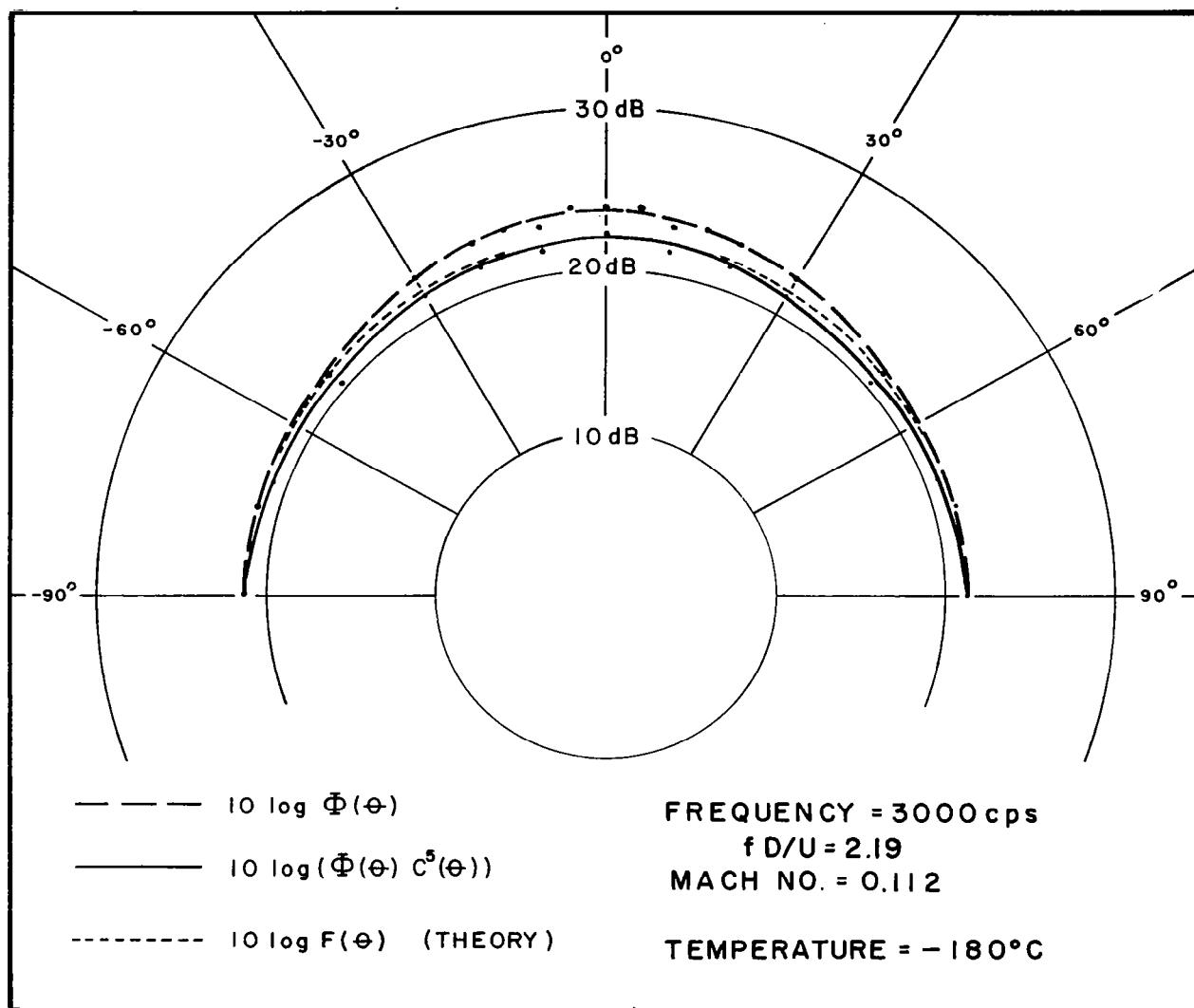


FIG.32. COMPARISON OF EXPERIMENTAL AND THEORETICAL BASIC DIRECTIVITY

*"The aeronautical and space activities of the United States shall be conducted so as to contribute . . . to the expansion of human knowledge of phenomena in the atmosphere and space. The Administration shall provide for the widest practicable and appropriate dissemination of information concerning its activities and the results thereof."*

—NATIONAL AERONAUTICS AND SPACE ACT OF 1958

## NASA SCIENTIFIC AND TECHNICAL PUBLICATIONS

**TECHNICAL REPORTS:** Scientific and technical information considered important, complete, and a lasting contribution to existing knowledge.

**TECHNICAL NOTES:** Information less broad in scope but nevertheless of importance as a contribution to existing knowledge.

**TECHNICAL MEMORANDUMS:** Information receiving limited distribution because of preliminary data, security classification, or other reasons.

**CONTRACTOR REPORTS:** Scientific and technical information generated under a NASA contract or grant and considered an important contribution to existing knowledge.

**TECHNICAL TRANSLATIONS:** Information published in a foreign language considered to merit NASA distribution in English.

**SPECIAL PUBLICATIONS:** Information derived from or of value to NASA activities. Publications include conference proceedings, monographs, data compilations, handbooks, sourcebooks, and special bibliographies.

**TECHNOLOGY UTILIZATION PUBLICATIONS:** Information on technology used by NASA that may be of particular interest in commercial and other non-aerospace applications. Publications include Tech Briefs, Technology Utilization Reports and Notes, and Technology Surveys.

*Details on the availability of these publications may be obtained from:*

SCIENTIFIC AND TECHNICAL INFORMATION DIVISION  
NATIONAL AERONAUTICS AND SPACE ADMINISTRATION  
Washington, D.C. 20546